

Università degli Studi di Napoli
“Federico II”

Facoltà di Scienze Matematiche Fisiche e Naturali

TESI DI DOTTORATO
IN
BIOLOGIA AVANZATA
XXII CICLO

*Disease-associated NEMO mutations as a tool to unravel the key
molecular mechanisms in NF-kappaB activation*

COORDINATORE:
Prof. Luciano Gaudio

CANDIDATA:
Dott.ssa Alessandra Pescatore

TUTOR:
Prof. Giuseppe Saccone

COTUTOR:
Dott.ssa Matilde Valeria Ursini

ANNO ACCADEMICO: 2008-2009

TABLE OF CONTENTS

1. INTRODUCTION	1
1.1 BACKGROUND	2
1.2 THE NF- κ B FAMILY MEMBERS	3
1.3 SIGNALING TO NF- κ B	3
1.4 THE I κ B KINASE COMPLEX: THE MASTER REGULATOR OF NF- κ B SIGNALING	5
1.5 UBIQUITIN-MEDIATED ACTIVATION OF IKK COMPLEX IN THE NF- κ B PATHWAY	8
1.5.1 THE UBIQUITINATION CODE	8
1.5.2 UBIQUITIN-MEDIATED ACTIVATION OF IKK COMPLEX	10
1.5.3 TRAFs: THE KEY INTERMEDIATES IN MOST NF- κ B PATHWAYS	13
1.6 INHERITED HUMAN GENETIC DISEASES CAUSED BY MUTATION IN THE NEMO GENE	14
1.6.1 THE INCONTINENTIA PIGMENTI	15
1.6.2 EDA-ID	16
2. AIM	18
3. METHODS	21
3.1 CASE REPORT	22
3.2 REAGENTS	22
3.3 MUTATION DETECTION AND X-INACTIVATION ANALYSIS	22
3.4 PLASMID CONSTRUCTION	23
3.5 CELL CULTURE	23
3.6 TRANSFECTIONS	23
3.7 RETROVIRAL INFECTIONS	25
3.8 IMMUNOPRECIPITATION AND WESTERN BLOTTING	25
4. RESULTS	27
4.1 <i>NEMO</i> MUTATIONS IN IP	28
4.2 MOLECULAR CHARACTERIZATION OF A NEW MISSENSE MUTATION OF <i>NEMO</i> CAUSING A SEVERE FORM OF INCONTINENTIA PIGMENTI	29
4.3 DEFECTIVE <i>NEMO</i> POLYUBIQUITINATION CAUSED BY A323P MUTATION	31
4.4 IDENTIFICATION OF TRAF-6-DEPENDENT <i>NEMO</i> UBIQUITINATION SITES	31
4.5 E57K: THE MASKED MUTANT	33
4.6 E57K IS DEFECTIVE IN TRAF6 BINDING	34
4.7 MAPPING THE TRAF6 BINDING SITE OF <i>NEMO</i>	35
4.8 THE LYSINE 90: THE CRITICAL RESIDUE FOR IKK COMPLEX FORMATION	36
5. DISCUSSION	38
6. REFERENCES	42
7. FIGURES	51

1. INTRODUCTION

1.1 Background

The Nuclear Factor (NF) κ B was first discovered in 1986 via its interaction with an 11-base pair sequence (GGGGACTTCC) in the immunoglobulin light-chain enhancer in B cells (κ B). Because it was constitutively present only in B cells in an appropriate stage for light chain expression, NF- κ B appeared to be a tissue-restricted transcription factor. However, it was shortly found in a masked cytoplasmic form in all mammalian cell types (Sen and Baltimore 1986).

Currently, the NF- κ B family proteins has been described and implicated in the inducible expression of a wide array of genes encoding proteins essential for innate and adaptive immunity, inflammation and cell survival (Gilmore 2006). Consistent with this role, mis-regulation of NF- κ B activity has been related to cancer, inflammatory and autoimmune diseases, viral infection and improper immune development. In addition, several human genetic diseases, affecting components of the NF- κ B signaling pathway, have been recently described.

The ample role of NF- κ B signaling in normal and disease physiology, is both its lure and its flaw as a therapeutic target.

1.2 The NF- κ B family members

The five NF- κ B family members share structural homology with the retroviral oncoprotein *v-Rel* and *Drosophila* dorsal gene products resulting in their classification as NF- κ B/Rel proteins (Gilmore 1999). All the members contain an N-terminus domain of approximately 300 amino acids called the Rel-homology domain (RHD), which mediates DNA binding, dimerization and nuclear localization. Generally, two subfamilies are distinguished: NF- κ B and the Rel proteins. The NF- κ B subfamily members named p50 and p52, which are the N-terminus fragments of the longer precursor NF- κ B1/p105 and NF- κ B2/p100 respectively, and the Rel subfamily members named RelA (p65), RelB and c-Rel, containing an unrelated C-terminus transcriptional activation domain, quite variable across species, even for a single Rel family member (Figure 1).

These proteins can homo- or heterodimerize to form either transcriptionally active (e.g., p50-p65) or repressive (e.g., p50-p50) dimers. Targeted disruption of all NF- κ B genes has been accomplished in mice, revealing a certain degree of redundancy among some of the family members. Mice lacking RelB develop normally to adulthood but display lack of lymph nodes and multi-focal defects in immune responses (Burkly, Hession et al. 1995; Weih, Carrasco et al. 1995). Mice lacking other NF- κ B proteins, including c-Rel and p52, have immune defects also (Kontgen, Grumont et al. 1995). However, there are also clear examples for exclusive roles of single Rel proteins. For instance, RelA-deficient mice die during embryogenesis because of massive, TNF α -induced apoptosis in the liver, demonstrating a vital, anti-apoptotic and unshared role of RelA (Hoffmann, Leung et al. 2003).

1.3 Signaling to NF- κ B

Activation of the NF- κ B signaling pathway is regulated at several

levels. Even so, the family of proteins called Inhibitor of κ B (I κ Bs) play a primary role in regulation of NF- κ B activity.

In the resting cells, NF- κ B dimers are retained as latent proteins through their association with I κ Bs. Following cell stimulation with any of a multitude of agonists, I κ B proteins are rapidly phosphorylated by the I κ B kinase complex (IKK), K-48 ubiquitinated and then degraded by the 26S proteasome (classically p65/p50-bound I κ B α). The freed NF- κ B dimers can move into the nucleus, where they bind to specific sequences in the promoter or enhancer regions of target genes (Figure 2) (Bonizzi and Karin 2004). Transcription of target genes is further regulated through posttranslational modifications of NF- κ B dimers that affect its ability to interact with transcriptional coactivators. NF- κ B-dependent transcription of I κ B proteins, as well as additional mechanisms targeting DNA-bound NF- κ B dimers, terminate the response (Hayden and Ghosh 2008).

In mammalian, three main members compose the I κ B family of proteins: I κ B α , I κ B β , I κ B ϵ . These proteins, characterized by the presence of multiple copies of ankyrin repeats (ANK), bound to NF- κ B dimers masking the Nuclear Localization Signal (NLS) present in its RHD, thereby preventing nuclear entry and DNA binding (Gilmore 2006). All of these I κ B proteins contain a conserved motif, near their N-termini, consisting of two serine residues, phosphorylated by IKK, and one or two lysine residues target of K-48-ubiquitination (Figure 1).

The precursor NF- κ B1/p105 and NF- κ B2/p100 contain the ankyrin repeats also, functioning as I κ B-like proteins maintaining their NF- κ B-subunit dimeric partners in the cytoplasm (Karin and Ben-Neriah 2000).

Furthermore, there are two “atypical” I κ B proteins called Bcl-3 (*BCL3*) and I κ B ζ (*NFKBZ*), which have inducible expression and appear to regulate NF- κ B by a distinct mechanism. It has been demonstrated that they interact with p50 and p52 containing complexes bound to the promoter and they can either inhibit or promote transcriptional responses (Hayden and Ghosh 2008).

A pivotal regulator of inducible NF- κ B signaling pathways is the I κ B kinase

(IKK) complex. This complex consists of two kinases, IKK1 (or IKK- α) and IKK2 (or IKK- β), and a regulatory subunit named NF- κ B essential modulator, NEMO (or IKK γ).

Genetic analysis of the IKK complex has identified two separate pathways named the canonical and non-canonical mechanisms that are dependent on either NEMO and IKK2 or IKK1 alone.

The non-canonical or “alternative” pathway operates mainly in B-cells in response to stimulation of a subset of the TNF-receptor superfamily, including receptors for BAFF, lymphotoxin- β (LT β) and CD40 ligand. Stimulation of these receptors results in the activation of the IKK α subunit that in turn phosphorylates the p100/p100 dimers, causing its inducible processing to the transcriptionally active form p52 (Xiao, Fong et al. 2004).

The principal NF- κ B signaling pathway is the “canonical”, that occurs upon the stimulation of many receptors such as the Toll-like Receptors (TLRs) in the innate immune response, T cell Receptor (TCR) in the adaptive immunity, TNF Receptor (TNFR) or Interleukin-1 Receptors (IL-1R) in inflammation or in response to a variety of endogenous ligands (such as viral DNAs or RNAs). Following ligand/receptor association, a complex cascade of events is activated. A wide range of adaptor and scaffolding proteins are recruited to the receptor preceding the activation of a number of intermediate kinases. Each signaling cascade employed unique or overlapping combinations of these upstream intermediates to transmit information from the cell surface to the NF- κ B-I κ B complexes.

Beside the variety of stimuli and molecules involved in the activation of “canonical” NF- κ B activation, the common feature is the activation of the IKK complex (Figure 2). Accordingly, it represents the core regulatory step in the NF- κ B response (Hayden and Ghosh 2008).

1.4 The I κ b Kinase complex: the master regulator of NF- κ B signaling

The pivotal IKK complex is the kinase complex responsible of I κ B protein phosphorylation. It is composed of two related catalytic subunits IKK1 (or IKK- α) and IKK2 (or IKK- β), of regulatory subunit NEMO (or IKK- γ) and accessory proteins such as Hsp90, cdc37 and ELKS, whose functions are either not NF- κ B specific whether fully characterized. By contrast to these IKK-associated proteins, the role of the core IKK subunits has been well established by a variety of genetic experiments, most importantly gene ablations in mice. Although both IKK1 and IKK2 are necessary for survival of mouse embryos, their respective roles in embryonic development and survival are quite different (Hayden and Ghosh 2008). IKK1 has a unique function in skin and skeletal development, as well as in B cell maturation, and its absence cannot be compensated for by IKK2 (Hu, Baud et al. 2001). In contrast, IKK2 appears to play an indispensable role in inducible NF- κ B activation in response to pro-inflammatory and pro-apoptotic stimuli. In absence of IKK2 embryonic lethality, liver degeneration is observed, similar to p65 knockout mice (Li, Chu et al. 1999). Severe liver degeneration and early lethality were also observed in embryos that were deficient in the NEMO subunit (Schmidt-Suppran, Bloch et al. 2000).

The two kinases share important structural identity and both contain an N-ter catalytic domain, a central leucine zipper motif through which they heterodimerize, a helix-loop-helix domain and a NEMO-Binding Domain at the C-terminus region (Figure 3). These proteins seem to have redundant functions, even if it has been shown that IKK2 is both necessary and sufficient for the phosphorylation of I κ B α on Ser32 and Ser36, and I κ B β on Ser19 and Ser23.

NEMO does not have enzymatic activity, although, genetic studies have clearly demonstrated that NEMO is necessary for a proper NF- κ B activation in response to most stimuli. NEMO is a 48kDa regulatory subunit that contains two coiled-coil motifs, denoted as CC1 and CC2, a Leucine Zipper and a Zinc Finger domain in the C-terminus region and a newly characterized Ubiquitin Binding Domain (UBD) that confers to NEMO the

ability to bind to polyubiquitinated proteins (Figure 3). CC1 domain overlaps with the IKK-binding domain (44-111aa), whereas the CC2-LZ and ZF domain play a regulatory role.

It has been proposed that multiple combinations of the IKK complex subunits exist including homodimers of IKK1 or IKK2 either associated or distinct from NEMO. The apparent molecular mass of the resting IKK complex has been shown to be in the 700-900 kDa range, suggesting that it may contain multiple copies of its constituents and that its size varies in a stimulus-dependent manner. However, biochemical evidence indicates that the majority of cellular IKK complexes contain a core of IKK1-IKK2-NEMO in the ratio of 1:1:2. NEMO exists as a partially folded dimer associated with the two kinases. Probably, the complex is maintained through multiple interactions with chaperone proteins like Hsp90, Hsp70 and CDC37 (Hayden and Ghosh 2008; Rushe, Silvan et al. 2008).

Current evidence show that the activation of the IKK complex is mediated by its recruitment to receptor-containing complex signalosomes, where, the final event for IKK activation seems to be its phosphorylation at specific Serines in the T loop of the catalytic domain of each kinases (Figure 3). Substitution of these serine residues with alanine makes both kinases catalytically inactive, whereas phosphomimic mutations in which the residues are substituted with glutamic acid generate constitutively active IKKs (Hacker and Karin 2006). The mechanism through which this phosphorylation occurs remains unclear, however, two mechanisms have been proposed. The first possibility is that the IKKs phosphorylates each other by transautophosphorylation. The second plausible mechanism could be the existence of unconnected kinases (IKK-Ks) that target the residues within the T loop. It is also possible that both mechanisms can occur independently or together in a manner that is dependent upon the nature of the specific upstream signaling pathway.

In contrast to this latter case, the critical role of NEMO for IKK-mediated activation has been definitively established.

NEMO is the point of convergence of most stimuli activating NF-

κ B, its interaction with signaling intermediates is essential for the correct IKK complex recruitment and activation. NEMO lacking cells fail to activate NF- κ B in response to proinflammatory cytokines such as Tumor Necrosis Factor (TNF)- α , Interleukin (IL)-1 and bacterial lipopolysaccharide (LPS). In addition, NEMO mutations have been associated to human genetic pathologies (discussed below).

NEMO interacts as a dimer together with IKK1 and IKK2, it can also oligomerize via a minimal oligomerization domain (MOD), constituted by the second CC region and the LZ domain (also called CoZi domain) (Agou, Courtois et al. 2004). It has been proposed that a change in the oligomeric state of NEMO may represent a recurrent mechanism of IKK activation, as mutations within the MOD can block IKK activation (Inohara, Koseki et al. 2000; Poyet, Srinivasula et al. 2000). Nevertheless, its oligomeric state still remains matter of controversy for the reason that a range of oligomeric states have been reported. Recent evidences demonstrated the existence of stimuli-induced posttranslational modifications of NEMO (discussed below) that could induce conformational change without variation in the stoichiometry of the complex composition.

Indeed, numerous proteins, producing either NF- κ B activation or inhibition, have been shown to interact with NEMO (Table 1) indicating that NEMO might act as a carrier responsible for bringing IKK-complex in close proximity to activators such as TGF β -activating kinase (TAK) to promote its phosphorylation and activation (Sebban, Yamaoka et al. 2006). NEMO also appears to control the downregulation phase of transient IKK activity. It has been demonstrated that NEMO serves as the docking platform for several negative regulatory proteins including the deubiquitinases A20 and CYLD (Kovalenko, Chable-Bessia et al. 2003) and the protein phosphatases PP2A and PP2C that may inhibit IKK activity by removing phosphates from the T loop serines (Fu, Kuo et al. 2003).

Several other proteins are also supposed to interact with NEMO but in most cases the functional relevance of this interaction is not precisely understood (Table 1).

Moreover, it has been recently shown that specific phosphorylation on Ser 68 of NEMO leads to downregulation of IKK activity, supporting a model in which IKK C-terminus autophosphorylation and phosphorylation of NEMO within the IKK-binding region leads to conformational changes that possibly recruit negative regulatory proteins to inhibit IKK function (Palkowitsch, Leidner et al. 2008).

1.5 Ubiquitin-Mediated Activation of IKK complex in the NF- κ B Pathway

1.5.1 The ubiquitination code

Ubiquitination has become a predominant topic in many fields of biology research, owing its role in regulation of various cellular processes. Ubiquitin (Ub) is a 76 aa highly conserved globular protein that is covalently attached to lysine (Lys) residues of target proteins. This covalent modification, known as ubiquitination, is carried out by a sequence of enzymatic reactions involving three main components. First, an ubiquitin activating enzyme (E1) uses ATP to catalyze the formation of a thioester bond between the C-terminus of ubiquitin and its active cysteine. Then, the latter ubiquitin is passed to a conjugating enzyme (E2 or UBC) forming an E2-ubiquitin thioester. Finally, ubiquitin is covalently attached to substrates through the formation of an isopeptide bond between the ubiquitin C-terminus and the ϵ -amino group of lysines on the target protein. The enzymes responsible for this last step, the ubiquitin ligases (E3), are the ones which provide target specificity by directly interacting with its substrates (Pickart 2004) (Figure 4A).

Depending on the E2/E3 machinery, mono- or polyubiquitination of proteins can be achieved. These two modifications are associated to different functional outcomes (Figure 4B).

Monoubiquitination is the attachment of a single ubiquitin to a protein; multiubiquitination occurs when several Lys residues of the target protein

are tagged with single Ub molecules. Monoubiquitination is an important modification and primarily serves to regulate the internalization of cell-surface proteins, intracellular protein sorting, and other cellular activities. Monoubiquitination of several residues on one substrate results in multiple monoubiquitination, which may promote subcellular relocalization or target substrates to the endosome- (as opposed to proteasome-) mediated degradation system (Mukhopadhyay and Riezman 2007).

Polyubiquitination consists in the addition of a polyubiquitin chain to the target protein. It is important to reiterate that the amino terminus of the group of lysine residues on ubiquitin may also serve as substrates for ubiquitination thus, the chain comprises several ubiquitins in which the C-terminus glycine residue of each ubiquitin is linked to a specific internal Lys of the previously attached ubiquitin. Because there are seven internal lysines in ubiquitin (K6, K11, K27, K29, K33, K48 and K63) at least seven different linkages between ubiquitins are possible (Ikeda and Dikic 2008) (Figure 4B).

The different linkages in polyubiquitin chains have different effects on the substrate and their role have begun to be elucidated in recent years. K48-linked polyubiquitinated chains are originally identified to deliver a “kiss of death” to the target protein, resulting in recognition and degradation by the 26S proteasome (Thrower, Hoffman et al. 2000). In contrast, when K63-linked polyubiquitinated chains are added to proteins no efficient degradation is observed but the target protein function is modified by various mechanisms (Geetha, Jiang et al. 2005). For instance, ubiquitination can provide a platform as three-dimensional signals for recruiting partners, an event which requires ubiquitin-binding (UB) proteins recognizing the specific patterns of ubiquitination on substrate proteins and direct the substrates to the appropriate fate (Figure 4B).

At present, close to 20 diverse types of UB Domains (UBDs), which are relatively different in terms of size, structure and function, have been identified (Hicke, Schubert et al. 2005). In this way, the distinct ubiquitin arrangements on substrates can promote specific outcomes.

Similar to phosphorylation, ubiquitination is a reversible process that is regulated at different levels. To this regard, the De-UBiquitination enzymes, (DUBs) that reverse the ubiquitin reaction, have an important role.

The ubiquitination event occurs in response to extra cellular stimuli and often the substrates are not constitutively recognized. Therefore, the activity of the ubiquitin system needs to be quickly and tightly regulated in order to increase specificity. This could be achieved by promoting or inhibiting substrate recognition.

Regulation can also occur through post-translational modification of a component of the ubiquitin conjugating machinery. Generally, the E3 ligases are the main component of the machinery subject to regulation. The two distinct E3 ligase family, the HECT-type and RING-type, both appear to be regulated by related modifications, e.g. ubiquitination and phosphorylation, that can either inhibit or promote E3 activity (Brown, Hostager et al. 2002; Yang, Zhou et al. 2006).

1.5.2 Ubiquitin-Mediated Activation of IKK complex

The multiplicity of ubiquitin role in protein kinase activation has been discovered in the course of studying the NF- κ B signaling pathway.

It was originally shown that the kinase activity could be started by polyubiquitination processes, which are different from the ones leading to protein degradation observed in the case of I κ B α (Chen, Parent et al. 1996). In the NF- κ B signaling, K63-linked ubiquitination has been observed to modify several distinct molecules participating in IKK activation. In addition, some components of signaling pathways leading to IKK/NF- κ B activation exhibit ubiquitin-binding properties (Table 2). This provides a complex framework of protein/protein interactions that is fine regulated by enzymes with deubiquitinating activity such as A20 and CYLD. In several instances, this framework has been elucidated to some extent.

The role of ubiquitin in IKK activation was first discovered in the course of studying the IL-1 signaling pathway. Upon stimulation of the IL-1 receptor

several proteins including the adaptor protein MyD88, the kinases IRAK1 and IRAK4, and TNF-R Associated Factor (TRAF) 6 are recruited to the receptor complex (Figure 5).

TRAF6 is an E3 ubiquitin ligase, containing a highly conserved N-ter RING domain, that catalyses K63-linked polyubiquitin chains (Deng, Wang et al. 2000). This K63 polyubiquitination seem to be an essential event leading the TAK kinase complex activation, probably by autophosphorylation, which in turn phosphorylates IKK2, resulting in IKK activation (Wang, Deng et al. 2001). The polyubiquitin chains, some of which are conjugated to TRAF6 itself, seem to function as scaffold to recruit TAK and IKK complex through binding the regulatory subunits, TAB2 and NEMO, respectively. The TAK1 kinase complex consists of TAK1 and its associated proteins TAB1 and TAB2 or TAB3 (Ishitani, Takaesu et al. 2003). TAB2 and TAB3 are homologous proteins that contain a C-terminus conserved UBD (NZF-type) conferring on TAB2 and TAB3 the ability to bind preferentially to K63 polyubiquitin chains. Mutations within the NZF domain that impair the ability of TAB2 and TAB3 to bind to polyubiquitin chains also abrogate their ability to activate TAK1 and IKK (Skaug, Jiang et al. 2009) (Table 2).

Likewise, NEMO represents an interesting case of K63 poliubiquitin chains recognition. Pull-down experiments have demonstrated that the region encompassing the second coiled-coil and the leucine zipper motifs (called NUB, NEMO Ubiquitin Binding domain, Figure 3) is unrelated to any other previously identified UBD, corresponds to an evolutionary conserved sequence which is also present in other proteins ABIN1-3 and Optineurin (Wagner, Carpentier et al. 2008). One physiological substrate of NEMO is receptor-interacting protein, RIP, which is indeed K63-ubiquitinated within minutes of TNFalfa stimulation. Mutation of the key Ub-acceptor lysines of RIP (K377) abrogates NEMO binding and subsequent IKK activation (Ea, Deng et al. 2006; Li, Kobayashi et al. 2006). Although NEMO and RIP can directly interact *in vitro* (Zhang, Kovalenko et al. 2000), the polyubiquitination of RIP upon TNF stimulation seems to

be the event determining their interaction *in vivo*. Recent studies, using an antibody specific for K63 polyubiquitin chains, have confirmed that RIP1 is conjugated by the K63 polyubiquitin chains following TNF α stimulation (Newton, Matsumoto et al. 2008). RIP1 is also K48-ubiquitinated and targeted for degradation by an ubiquitin complex containing the deubiquitination enzyme A20. It has been proposed that NEMO protects RIP1 from the proteasomal degradation by preventing the conversion of K63-linked to K48-linked polyubiquitination promoted by the A20 protein. Also in this case, the function of the polyubiquitin chain on RIP1 appears to be the recruitment of the TAK1 and the IKK complexes to the TNFR. This mechanism of recruitment to RIP1 may serve as a paradigm for the role of K63-linked ubiquitin in the NF- κ B pathway providing an elegant and compelling model that can be expanded to other pathways, including those involving TLR that operates by similar ways and differs principally in the TRAFs paralogue used (Figure 5).

Although these evidences highlight the importance of ubiquitin binding in kinase regulation, the mechanism by which binding to polyubiquitinated proteins leads to the activation of kinase complex remains to be elucidated. Structural studies about NEMO and TAB2 UBDs will provide important informations to propose a definitive model of activation. Interestingly, the importance of ubiquitination in the IKK activation is also underlined by the significant role of DUB enzymes, such as CYLD and A20, which disassemble K63 polyubiquitin chains to inhibit the signaling cascade.

CYLD is the first DUB discovered to negatively regulate TRAFs induced IKK activation (Kovalenko, Chable-Bessia et al. 2003). Mutations in CYLD have been identified in patients with familial cylindromatosis in which affected individuals develop multiple benign tumors of the skin appendages. (Bignell, Warren et al. 2000). This combination of genetic and biochemical evidence strongly suggests that ubiquitin-mediated regulation of IKK activation has a critical role in human physiology and that its misregulation can have devastating consequences.

Adding another level of complexity to the mechanism(s) of IKK complex activation, it has been demonstrated that NEMO may also be a target for K63-linked polyubiquitination in a variety of signaling cascades. This event appears to have an impact on its function (Figure 5). TNF stimulation induces NEMO K63-linked polyubiquitination probably mediated by TRAF2 and cIAPs. Mutations in the NEMO ZF domain also impair the ubiquitination event (Tang, Wang et al. 2003).

Engagement of the TCR- and BCR also induces NEMO ubiquitination, in this case MALT-1 is the E3 ligase responsible for both its mode of action and its functional relationship to TRAF-2 and TRAF-6, which seem also to participate in TCR and BCR signaling (Sun, Deng et al. 2004).

1.5.3 TRAFs: The key intermediates in most NF- κ B pathways

TRAFs [tumor necrosis factor (TNF) receptor (TNFR)-associated factors] are a family of seven proteins that have important roles in signal transduction of TNFR and IL-1 receptor (IL-1R) toll-like receptor (TLR) superfamilies and B cell receptor (BCR). A wide range of biological functions, such as inflammatory response, immunity, and bone metabolism, rely on the proper functions of TRAF proteins to activate IKK complex and MAP kinases, leading to activation of NF- κ B and AP-1 respectively.

All TRAF proteins, except TRAF7, contain at C-terminus TRAF domain which contains a TRAF-N domain predicted form a coiled coil and an highly conserved TRAF-C domain, which mediates homo- and hetero-dimerization, as well as their association with members of the TNFR and IL-1R–TLR receptor families (Park, Burkitt et al. 1999). Two additional functional domains at the N terminus, a variable number of zinc fingers domain and the RING domain, are shared by TRAF2–TRAF7.

The RING domain is important for downstream signaling by TRAF proteins. Unlike most E3s containing the RING domain, the primary function of TRAF2 and TRAF6 is not to target protein for degradation but to activate downstream IKK cascades (Deng, Wang et al. 2000). These

TRAF proteins function in conjunction with the Ub-conjugating enzyme (E2) to catalyze the formation of K63-linked polyubiquitin chain. They do not seem to have catalytic activity but provide a connection between E2s and the substrate. Notably, TRAF2, 3 and 5 seem to contribute only in TNF receptor signal transduction while, TRAF6 has been implicated in the transduction of many receptor signals (Pineda, Ea et al. 2007), including Toll and IL-1 receptor. TRAF2 and TRAF6 overexpression is sufficient to induce activation of the canonical NF- κ B pathway. Biochemical studies demonstrated that TRAF6 (and TRAF2 also) is subject to self-polyubiquitination (K63), revealing a critical role of this kind of posttranslational modification (Lamothe, Besse et al. 2007; Lamothe, Campos et al. 2008). However, the exact mechanism by which these proteins act is still unclear.

1.6 Inherited human genetic diseases caused by mutation in the NEMO gene

The human gene encoding NEMO, the *Inhibitor of Kappa light polypeptide gene enhancer in B-cells, Kinase Gamma (IKBKG; NM_003639.3)*, is a 23 Kilo base (Kb) gene structured in 9 exons and 4 alternative non coding first exons located on the X chromosome (Xq28) (Smahi, Courtois et al. 2000).

NEMO mutations have been associated with several distinct X-linked genetic diseases.

1.6.1 The Incontinentia Pigmenti

Incontinentia Pigmenti (IP; OMIM#308300) is the first genetic disease associated to NF- κ B alteration. IP is a severe X-linked dominant genodermatosis which is lethal in males (Landy and Donnai 1993) and in females has a highly variable and often severe clinical presentation always associated with skin defects characterised by four distinct dermatological

stages. IP female patients can also suffer from severe ophthalmological, odontological or neurological defects (Hadj-Rabia, Froidevaux et al. 2003). A very striking feature of the IP pathology is the extensive X inactivation skewing that is observed in the peripheral blood cells of heterozygous IP females (Fusco, Bardaro et al. 2004).

The gene responsible for IP, *NEMO*, is mutated in 73% of IP patients screened. It encodes for the regulatory subunit of the Inhibitor of KappaB Kinase (IKK) complex (NEMO) required for a proper NF- κ B activation (Smahi, Courtois et al. 2000). IP is the first described inherited disease associated with mutations affecting one of the core components of the NF- κ B signaling pathway.

In IP patients, a recurrent deletion occurs. This rearrangement leads to an excision of the region between two ME_{DIUM} REITERATED 67B (MER67B) repeated sequences, producing an aberrant protein in which 26 novel amino acids are attached to the 133 residues encoded by exons 2 and 3. As a result, cells from rearranged IP patients do not activate NF- κ B in response to cytokines and are highly sensitive to TNF- α -induced apoptosis (Aradhya, Woffendin et al. 2001).

Besides the exon 4_10 rearrangement, other *NEMO* mutations have been identified (small duplications, substitutions or deletions) scattered along the gene. Although many of them such as nonsense or frameshift mutations result in a large truncation or extension of the NEMO protein, several missense mutations have also been reported. The observation that IP-causing mutations affect all exons of the *NEMO* gene is consistent with the importance of the entire amino acid sequence for its function.

The phenotype of IP patients is difficult to interpret, owing to the X-mosaicism. Schmidt-Supprian and colleagues have engineered *Nemo* knockout mice (KO) (Schmidt-Supprian, Bloch et al. 2000). Male mice die very early during embryogenesis from massive liver apoptosis triggered by TNF- α . In contrast to males, KO female mice develop normally but, soon after birth, exhibit patchy skin lesions with massive granulocyte infiltration. Similar to IP patients the lesions are associated with hyperproliferation and

increased apoptosis of keratinocytes. In addition, the extensive X-inactivation skewing in blood leukocytes is also observed in *Nemo* KO mice.

The data collected from the mouse models could provide a putative explanation for the IP phenotype. In most cells, such as circulating blood cells or hepatocytes, X-inactivation appears severely skewed, because of selection against cells carrying the *NEMO* mutated locus. Probably, at the skin level, elimination of mutated cells starts only after birth generating dermatosis observed in all IP patients. The initial signals triggering this event is still unknown, probably certain kind of stress might induce necrosis of Nemo (-) keratinocytes. This would cause a local inflammation response and the secretion of cytokines, such as TNF- α . As a consequence, NEMO lacking cells would die as a result of TNF- α -induced apoptosis, caused by a complete abolition of the NF- κ B signaling pathway (Sebban and Courtois 2006) (Figure 6).

1.6.2 EDA-ID

Genetic studies have revealed that IP is allelic with an X-Recessive Immunodeficiency syndrome termed Anhydrotic Ectodermal Dysplasia with severe ImmunoDeficiency (EDA-ID, OMIM#300291), a very rare disease exclusively affecting males. It combines the severe sensitivity to infection with abnormal development of skin adnexa (hair follicles, sweat glands and teeth). This disease is due to *NEMO* hypomorphic mutations, often missense or small deletions/insertions, which mainly affect the Zinc Finger (ZF) domain of the protein. These mutations reduce but do not eliminate NF- κ B activation explaining why affected male patients survive (Zonana, Elder et al. 2000; Doffinger, Smahi et al. 2001; Kenwrick, Woffendin et al. 2001)

A quite remarkable difference in clinical signs has been observed between IP females and EDA-ID males. This diversity could be due to the different type and location of the mutations that cause the two diseases, but also to the mosaic expression of *NEMO* due to random X inactivation in

heterozygous females. Indeed, a rapid progressive selection against peripheral blood cells carrying the mutated X-chromosome can explain why IP patients do not suffer from immunodeficiency while EDA-ID patients always present a severe sensitivity to infections (Courtois and Gilmore 2006).

2. *AIM*

NF- κ B is an ubiquitous transcription factor involved in a variety of biological processes, such as inflammation, immunity, cell survival and development. In the resting cells NF- κ B dimers are retained as latent protein through their association with I κ B. In response to several stimuli, such as pro-inflammatory cytokines, NF- κ B dimers became active translocating to the nucleus, where they bind to specific sequences in the promoter or enhancer regions of target genes.

The NF- κ B signaling pathways emanating from the TNFR receptors IL1R and TCR4 have been most studied. In NF- κ B canonical activation, following ligand/receptor interaction, adaptor molecules and kinases are recruited to the receptor and all the signals converge on the pivotal IKK complex, which is composed by two related catalytic subunits, IKK1 and IKK2, and a regulatory subunit called NEMO. One of the main questions about the activation of NF- κ B is how the IKK-complex is activated. To this regard, the central role of NEMO in mediating canonical NF- κ B activation pathways has been largely demonstrated through biochemical and genetic studies but how NEMO can integrate the various signaling pathways regulating the activity of IKK complex is still unknown.

The whole amino acid sequence of NEMO is required for a correct assembly and recruitment of the IKK complex to upstream signaling molecules. Supporting this view, numerous proteins producing either NF- κ B activation or inhibition have been shown to interact with NEMO and in turn, regulate the IKK activity. Furthermore, several lines of evidences have revealed the existence of many regulatory posttranslational modifications of NEMO, e.g. K63-linked polyubiquitination, that occur in response to specific stimuli at specific sites and seem to be essential for its function (Sebban, Yamaoka et al. 2006). Despite their indispensability in several pathways, the precise mechanisms by which NEMO activity is regulated by posttranslational modification remain unclear.

Given the critical role of NEMO, it is not a surprise that NEMO mutations are causative of human diseases. The first described is Incontinentia Pigmenti (IP), an X-linked dominant and male-lethal disease.

Heterozygous IP females can survive owing to X-inactivation mosaicism and present neonatal rash, and frequently malformations of eyes, teeth and central nervous system. The overall objective of my thesis is to contribute in ameliorate our understanding of the genetic and pathological aspects of NEMO-related diseases. In order to get insights into the molecular mechanisms that underline the alteration of NF- κ B during pathology, we combined the characterization of human disease-associated mutations with the elucidation of the IKK activation process NEMO-dependent. To date, only few NEMO missense mutations have been characterized at functional level. Through the molecular characterization of missense mutations I will define the critical residues of NEMO required for proper protein/protein interaction and/or the specific residues that are target of regulatory modifications, e.g. K-63 polyubiquitination, essential for a correct signal transduction.

Importantly, a better understanding of IP at the cellular and molecular levels could offer useful information to dissect the NF- κ B regulation in order to propose new therapeutic options, not only for this specific pathology but also for more common pathologies resulting from NF- κ B dysfunction.

3. METHODS

3.1 Case report

Patient KB is a 12 year old female who developed cutaneous rash with vesicles on the trunk and the limbs (first stage of IP) at 1 month of age. Those vesicles then became hyperkeratotic warty lesions (second stage) at 3 months of age. In the third stage, pigmented spots appeared in linear and whorled pattern on the trunk and the limbs (at 1 year), while the fourth stage has not appeared at the time of the *NEMO* molecular analysis. Skin biopsies performed at the first stage confirmed marked dyskeratosis and eosinophilic infiltration consistent with IP.

No alterations were observed in the hair, fingernails and eyes. In contrast, neurological alterations were present: microcephaly, brain atrophy, were diagnosed at birth and at the same time CT scan analysis showed severe cortico-subcortical atrophy, mostly in the left hemisphere. Neonatal seizures were observed at the time of IP diagnosis (1 month of age). Mental retardation and learning difficulties were diagnosed at 3 years.

The patient is the second child in the family with 4 siblings. However, the other members of the family, parents and 3 siblings, were examined and nobody was IP affected.

3.2 Reagents

The following antibodies were used: anti-human NEMO (sc-8330 Santa-Cruz), anti-mouse NEMO (#3329, a kind gift of N. Rice), anti-IKK-1 (Imgenex), anti-IKK-2 (Imgenex), anti-RIP (Imgenex), anti-TRAF-6 (sc-7221, Santa-Cruz), anti-RICK (sc-22763, Santa-Cruz) and anti-phospho-JNK (Cell Signaling), TNF- α and IL-1 β were from Roche and Peprotech, LPS and LPA were from Sigma.

3.3 Mutation detection and X-inactivation analysis

Mutation G967C of *NEMO* was identified and X-inactivation skewing was measured using protocols described previously for other *NEMO* mutations (Fusco, Bardaro et al. 2004).

3.4 Plasmid construction

The full-length human NEMO cDNA was inserted between the Hind III and Not I sites of the pcDNA3 vector. I generated plasmids carrying the point-mutations found in IP patients using the Quick-change site-directed mutagenesis kit (Stratagene). The sequence of all the mutated constructs was checked by automatic directed sequencing, using T7 and Sp6 primers. The same procedure was used to prepare all the point mutations in the full length version of mNEMO, previously inserted into a pcDNA3-HA expression vector. The truncated versions of mNEMO (dN241, dC385, dC343 and dC299) were generated by PCR and inserted into pcDNA3-HA. The pBabe-NEMO plasmid and its mutants were produced by PCR .

3.5 Cell culture

HEK293T, Mefs and LinX cells were maintained in Dulbecco's modified Eagle's medium (DMEM, Invitrogen, Carlsbad, CA) supplemented with 10% fetal bovine serum, 100 U/ml penicillin, 100mg/ml streptomycin and 1% glutamine at 37°C in 5% CO₂. 1,3E2 cells were grown in RPMI (GIBCO) containing 10% fetal bovine serum, 1%, antibiotics (100 U/ml penicillin, 100 mg/ml streptomycin) and 50 µM β-mercaptoethanol at 37°C in 5% CO₂.

3.6 Transfections

1.3E2 cells were transfected using DEAE-Dextran, as previously described (26). Transfection of SVT-2C cells was performed similarly. Briefly, 5×10^6 cells were washed in TBS (25 mM Tris-HCl (pH 7.4), 137 mM NaCl, 5 mM KCl, 0.6 mM Na_2HPO_4 , 0.7 mM CaCl_2 , 0.5 mM MgCl_2), resuspended in 250 μl of TBS, and NEMO expression plasmid (200 ng), Igk-Luc reporter plasmid (1 μg) and internal control eF1-LacZ (200 ng) were added. Cells were finally mixed with 250 μl of DEAE-Dextran (1 mg/ml, diluted in TBS). After 45 min of incubation at room temperature, cells were diluted with 5 ml of TBS, centrifuged and resuspended in 5 ml of RPMI/10% FCS. Twenty-four hours later cells were recovered in 100 μl of Lysis Buffer (LB) (25 mM Tris-phosphate (pH 7.8), 8 mM MgCl_2 , 1 mM DTT, Triton X100, 25% glycerol) and luciferase activity was assessed using the Luciferase Assay system (Promega). Transfection of NEMO (-) MEFs was carried out by electroporation. Briefly, the cell equivalent of a confluent 10 cm^2 dish was resuspended in 300 μl of PBS and 100 μl were electroporated (500 μF , 160V, Gene Pulser X-cell Electroporation System, BioRad) after adding 1 μg of reporter plasmid, 200 ng of eF1-LacZ and 500 ng of NEMO expression vector. After electroporation, cells were resuspended in 9 ml of DMEM/10% FCS and used to fill 3 wells of a 6 well dish. The morning after, the medium was changed. In the evening, cells were serum starved by adding DMEM without FCS. After 16 h of starvation, cells were mock-, TNF- (10 ng/ml), IL-1- (10 ng/ml) or LPS- (15 $\mu\text{g}/\text{ml}$) stimulated. Four hours later, cells were lysed with LB and luciferase was measured as described above.

Transfection of NEMO (-) MEFs was carried out also using Lipofectamine 2000 mediated transfections, according to the manufacturer's instructions (Invitrogen). All transfections included supplemental empty vector to ensure that the total amount of transfected DNA was kept constant in each dish culture.

Transfection of HEK 293T cells in 6-well dishes was carried out using a standard Calcium Phosphate procedure. In each transfection protocol, an internal control (eF1-lacZ) was included to correct for variations between

the samples (Kovalenko, Chable-Bessia et al. 2003). β -galactosidase activity was measured using Luminescent β -galactosidase Reporter System 3 from Clontech.

3.7 Retroviral Infections

Gene transfer was achieved by a retrovirus-mediated process. The retrovirus pBabe-NEMO, its mutant forms and control pBabe-puro were used to infect Mefs NEMO (-) cells. Cell lines expressing NEMO and its mutants were selected along with a pBabe-puro control line. The expression of NEMO was detected by immunoblot analysis.

The pBabe-NEMO plasmids and empty pBabe-puro were used to transfect LinX packaging cells, using the standard CaPO3 procedure. Conditioned media (48-hour culture) collected from the transfected LinX cells were filtered through a 0.45- μ m pore size syringe filter. The viral supernatants were mixed with defined DMEM (1:1). This mixture, supplemented with polybrene (8 μ g/mL), was added to recipient cells, Mefs Nemo(-/-), that had been plated at 5×10^5 cells per 100-mm dish the day before infection. Mefs cells were cultured in viral supernatants for 10 hours followed by 12 hours in DMEM supplemented with 10% fetal bovine serum, 100 U/ml penicillin, 100mg/ml streptomycin. After 12h the cells were subjected to selection in 2 μ g/mL puromycin for 14 to 21 days. A pool of puromycin-resistant cells was obtained. The selected cells were then maintained in a defined Mefs medium.

3.8 Immunoprecipitation and Western blotting

HEK 293T cells transfected were recovered by gentle pipeting in 1 ml of PBS. They were centrifuged at 6000 rpm for 1min in a microfuge and resuspended in 50-100 μ l of TNT buffer (200 mM NaCl, 1 % Triton X-100, 20 mM Tris-HCl, pH 7.5). After incubation on ice for 10 min and

centrifugation at 14000 rpm for 10 min, the supernatant was recovered and the protein concentration determined. One hundred to 200 μg of proteins (in 200 μl of TNT) were either directly analyzed, after electrophoresis, by Western blotting (see below) or immunoprecipitated. In this latter case, extracts were incubated under rotation for 1h at 4°C with the relevant antibody. Protein A- or protein G-Sepharose was then added and the mixture incubated for 30 more min at 4°C. Sepharose beads were quickly centrifuged in a microfuge (30s at 14000 rpm) and washed four times with TNT. After the final wash, the beads were resuspended in 30 μl of Buffer A (10 mM KCl, 2 mM MgCl₂, 0.1 mM EDTA, 1 mM DTT, 10 mM Hepes (pH 7,8)). For immunoprecipitation of transfected proteins, MEFs cells were transiently transfected and 24 h after transfection cells were lysed in Triton X-100 lysis buffer (20mM Hepes, pH 7.4, 150 mM NaCl, 10% glycerol, 1% Triton X-100, and Complete Protease Inhibitor mixture). After an additional 10 min on ice, cell extracts were centrifuged for 10 min at 14,000g at 4°C and supernatants were incubated for 4 h at 4°C with anti-FLAG antibodies bound to agarose beads (M2, Sigma). The immunoprecipitates were washed five times with Triton X-100 lysis buffer and subjected to SDS–PAGE. Gels were transferred at 100 V for 1h onto Immun-Blot PVDF membranes (BioRad) which were blocked in 4% dry milk/PBS for 1h. Incubation with the relevant Ab was carried out in 0.4% dry milk/PBS for 1h. The membrane was washed three times in 0.05 % Tween/PBS for 10 min and incubated with the secondary HPR-linked antibody for 45 min in 0.4 % dry milk/PBS. After the final washes, membranes were analyzed using either ECL + (Amersham) or SuperSignal West Pico Chemiluminescent Kit (Pierce).

4. RESULTS

4.1 *NEMO* mutations in IP

Between 70 and 80% of IP patients exhibit the same genomic rearrangement that deletes the locus encoding *NEMO*.

The most frequent mutation in females IP is the exon4_10 deletion (c.399-?_1260+?del) which occurs between two identical MER67B repeats (Figure 7). This recurrent deletion (c.399-?_1260+?del) eliminates ~11kb of the *NEMO* gene (also called *IKBKG*) and it is lethal in males.

Considering the data that have been published during the last eight years a total of 47 different mutations have been described: 27 are frameshift, 11 are nonsense, 2 are splice site mutations and one is a nonstop mutation. Among the remaining patients only few small mutations (5 missense and 1 in frame deletion of one codon) of *NEMO* have been described. Most of the missense mutations found in IP affect residues conserved in vertebrates during evolution (Table 3)(Fusco, Pescatore et al. 2008).

The overall mutation detection rate in IP is 73%. However, extensive research is still in progress to identify new genomic rearrangements, which may account for the remaining 27% of IP patients without the *NEMO* mutation. The *NEMO* region in humans is particularly full of repetitive sequences and therefore must be considered a *rearrangement-prone* region (Aradhya, Bardaro et al. 2001). A non-functional partial second copy of the *NEMO* gene, *deltaNEMO*, is located 31.6 Kb distal to exon10 (Figure 7). *NEMO* maps within a 35.5 Kb duplicated fragment (>99% identity) opposite to *NEMO* in orientation. It contains the exons 3-10 and carries the two MER67B repeats, which also may recombine (Aradhya, Bardaro et al. 2001). Although, no evidence of an involvement of the *NEMO* pseudogene in human diseases has so far been reported, the non-pathological exon 4_10 deletion of *deltaNEMO* has been found in two families, in unaffected parents of females with a clinical diagnosis of IP. As a consequence, to formulate a correct molecular diagnosis of IP is important to discriminate between mutations occurring in *NEMO* or in its pseudogene. Indeed, the IP locus undergoes recombination producing benign variants that might be “at

risk'' of generating *de novo* *NEMO* deletion during either meiotic or mitotic division (Fusco, Paciolla et al. 2009).

The molecular characterization of missense mutations may provide precious info regarding the *in vivo* function of *NEMO* in NF- κ B signalling.

The first mutation I decided to analyze is a new mutation, a G to C transversion mutation at nucleotide 967 (numbered from the ATG initiation codon), which results in a substitution of Alanine 323 in a Proine mutation (A323P) located at the beginning of the leucine zipper (LZ) of *NEMO* protein. Furthermore, I analyzed other mutations of *NEMO* (E57K, DK90, D113N and R123W) that have been recently described and are located within the first 150 aa of the protein, encompassing the region of IKK binding domain (Table 3).

4.2 Molecular characterization of a new missense mutation of *NEMO* causing a severe form of Incontinentia Pigmenti

In the Dr. Ursini's Lab, we sequenced the *NEMO* gene of a newborn girl exhibiting a severe form of IP associated with neurological abnormalities (see « Case Report » in the Material and Methods section). A heterozygous G to C transversion mutation at nucleotide 967 (numbered from the ATG initiation codon) was found, which resulted in a missense mutation (A323P) located at the beginning of the *NEMO* leucine zipper (Figure 8A).

X-inactivation skewing in the proband's peripheral blood cells was above 90% (Figure 8A), as observed in most IP cases, precluding any study of cells directly derived from the patient. In order to evaluate the impact of the mutation on NF- κ B signaling I took advantage of the recent isolation and characterization of several cell lines lacking *NEMO* to complement them transiently with a plasmid expressing A323P *NEMO* and to analyze their response to several stimuli, among them TNF, IL-1, LPS and PMA/Ionomycine. Two of these cell lines, 1.3E2 and SVT-2C, are

lymphocytes of the murine pre-B and human T-cell lineage, respectively (Courtois, Whiteside et al. 1997; Harhaj, Good et al. 2000; Schmidt-Supprian, Bloch et al. 2000), whereas NEMO (-) MEFs are fibroblasts that have been derived from a mouse model of IP (Schmidt-Supprian, Bloch et al. 2000)

In the two cell types in which I carried out the analysis, SVT-2C and NEMO (-) MEFs, an abolished activation of an NF- κ B reporter gene in response to TNF was observed after expressing A323P NEMO (Figure 8B). In addition, a strong reduction of activation was detected when NEMO (-) MEFs were transfected with A323P NEMO and stimulated with IL-1. Finally, in 1.3E2 cells, I checked the effect of A323P mutation on NF- κ B activation induced by LPS stimulation. Again, an impaired response was observed. Although defective TCR signaling is not observed in IP patients, because of the efficient chromosome X-driven elimination of T lymphocytes harboring *NEMO* mutations, I wondered whether this pathway was also affected by A323P mutation. Whereas transient complementation of SVT-2C cells with wt NEMO followed by PMA/Ionomycin stimulation resulted in potent NF- κ B activation no such activation was seen upon complementation with A323P mutation (Figure 8B). From this set of data I could conclude that A323P mutation exhibited a strong defect in NF- κ B signaling affecting several distinct signaling pathways. Importantly, this aspect was not caused by some major structural alteration of the NEMO molecule since A323P mutation did not show any defective interaction with previously identified partners such as IKK-2 or RIP, as assessed by performing co-transfection experiments and immunoprecipitations in HEK 293T cells (Figure 9A, B).

All the complementation experiments described above were carried out by transiently transfecting cell lines, a method that did not allow to detect expression of the molecules produced after transfection. To exclude any general impairment in NF- κ B activation resulting from instability of the NEMO protein I generated stable cell lines expressing either wt or A323P NEMO proteins. As shown in Figure 8C, pools of SVT-2C cells expressed WT or A323P NEMO at a similar level, demonstrating that the mutated

protein was stable. Moreover, normal incorporation of A323P NEMO into the IKK complex was confirmed by co-immunoprecipitating a similar amount of IKK1 and IKK2 as with wt NEMO (Figure 8C, 9A). From this set of data, I concluded that A323P mutation exhibited a specific impairment affecting at least two distinct pathways of NF- κ B activation, the TNF and the IL-1/TLR signaling pathways, that bear relevance to the phenotype developed by IP patients.

4.3 Defective NEMO polyubiquitination caused by A323P mutation

It has previously shown that co-transfecting plasmids expressing NEMO and ubiquitin in 293T cells results in NEMO K63-linked polyubiquitination and that this kind of modification does not regulate the stability of this protein but may, through an unclear mechanism, regulate its function. Interestingly, when A323P NEMO ubiquitination was monitored using this specific assay a severe reduction in ubiquitination was observed (Figure 10A). I therefore invested some efforts in trying to identify which pathway may be responsible for this basal ubiquitination process. To a large extent, NEMO ubiquitination was diminished upon co-transfection of a dominant negative version of TRAF-6, something that was not observed using a dominant negative version of TRAF-2 (Figure 10B). This suggested that some TRAF-6 dependent pathway may be responsible for NEMO ubiquitination. Accordingly, when TRAF-6 was co-expressed with both wt NEMO and ubiquitin, a strong increase in NEMO ubiquitination was observed. In this assay again, A323P mutation exhibited defective ubiquitination (Figure 10C).

4.4 Identification of TRAF-6-dependent NEMO ubiquitination sites

The observation that TRAF-6-dependent ubiquitination of NEMO

was impaired upon mutation of A323 suggested that this may provide a clue to identify the specific lysine residues targeted by TRAF-6.

To independently confirm that the region of NEMO containing A323P mutation indeed provided ubiquitination sites for TRAF6, a deletion analysis was also carried out, using either C-ter or N-ter truncations of the murine protein. This analysis of TRAF6-mediated ubiquitination confirmed the existence of ubiquitination sites between aa 343 and aa 299 (Figure 12A).

For practical reasons, all the follow experiments were performed using mouse NEMO, after confirming that V316P mutation behaved equivalently to human A323P mutation (Figure 11A). As shown on Figure 11B, two conserved lysines (hK321 and hK326, human coordinates; mK314 and mK319, mouse coordinates) are located in close proximity to hAla 323 (mVal 316) and could be affected by the appearance of a Proline nearby. To check for this possibility, experiments were carried out as described above, using a triple mutation targeting the mK318, mK319, mK314 (K was mutated in R, mutant 3R). A defective ubiquitination was found despite mutant 3R did not completely abolish TRAF-6-induced NEMO ubiquitination, suggesting the existence of additional acceptor sites (Figure 12B).

Interestingly, a lysine residue of NEMO modified by the Nod2/RICK signaling pathway, which is perturbed in Crohn disease, has been identified at hK285 (Abbott, Yang et al. 2007). Moreover, the E3 ligase used by Nod2/RICK to ubiquitinate this site has not been defined. I therefore tested the possibility that it may represent an additional target of TRAF-6 since, as mentioned above, I observed some residual NEMO ubiquitination taking place upstream of aa 299. Accordingly, the residual ubiquitination of 3R was almost totally abolished upon mutating mK278 also (construct 4R) (Figure 12B).

Having identified several distinct lysines of NEMO that may represent sites for TRAF-6-dependent polyubiquitination I investigated the impact of their mutation on NF- κ B signaling.

I first analyzed 3R or 4R mutants on the activation of NF- κ B by IL-1, which is a prototypical cytokine using TRAF-6 E3 ligase. Since defective TRAF-6 mediated ubiquitination of NEMO requires the mutation of several of these residues (see above), In both mutants 3R and 4R a 40% of reduction in NF- κ B activation was observed. In the same assay, activation of NF- κ B by TNF was not significantly affected by mutation 4R, indicating that the newly identified sites of ubiquitination were specifically required by a stimulus using TRAF6 (Figure 13).

I next checked whether other signaling pathways known to activate NF- κ B through TRAF-6 were also dependent upon NEMO ubiquitination. Activation of NF- κ B by LPS, which relies upon a TLR-dependent signaling pathway was more than 60 % impaired when NEMO (-) MEFs were complemented with 5R mutant (mutating residue mK392, which has been reported involved in the TCR signaling, in construct 4R) (Figure 13).

I finally analyzed the contribution of NEMO ubiquitination to pathways that remain less well characterized but might also require TRAF-6.

Very recently, a participation of Bcl10/MALT-1 in NF- κ B activation by LPA, a major component of serum exhibiting mitogenic properties, has been reported (Klemm, Zimmermann et al. 2007). Importantly, Bcl10/MALT-1 complex appears to act through TRAF-6. I therefore analyzed whether TRAF-6-dependent NEMO ubiquitination was involved in serum- and LPA-induced NF- κ B activation. The activation of NF- κ B was compromised when NEMO (-) MEFs were complemented with 5R mutant (Figure 13). This indicates that NEMO ubiquitination also plays an essential role in serum-induced NF- κ B activation.

4.5 E57K: the masked mutant

In order to evaluate the impact of the E57K mutation on NF- κ B signaling, I transiently complement cell lines lacking NEMO with a plasmid expressing E57K NEMO and I analyzed its response to several stimuli, among them TNF, IL-1, LPS. Despite repeated attempts, I was unable to

detect any reproducible reduction of NF- κ B activation in response to IL-1 or LPS when NEMO (-) 1.3E2 cells or NEMO (-) MEFs were transiently complemented with E57K NEMO (data not shown). This mutation has been associated with a mild form of IP so, to further investigate if E57K NEMO really affected the IL-1 pathway, I generated stably MEFs NEMO (-) expressing WT NEMO or E57K NEMO at physiological levels. This allowed me to discover its putative effect on NF- κ B signaling. As shown in Figure 14A, pools of MEFs expressing identical level wt or E57K NEMO were obtained after retroviral infection (lower panel). The protein expression level was similar to the endogenous NEMO in wt MEFs, confirming the stability of E57K NEMO protein.

I next investigated the effect of E57K NEMO on NF- κ B activation. Upon treatment with IL-1, NF- κ B activation in E57K-expressing cells appeared reduced (approximately 45%) compared to wt NEMO-expressing cells (Figure 14A). Moreover, activation of NF- κ B following TRAF6 overexpression was also reduced (Figure 14A), indicating a specific defect involving this E3 ubiquitin ligase. Finally, mutation E57K did not impair NF- κ B activation when TNF was used as a stimulus. This suggested that E57K mutation found in IP was specifically associated with impaired NF- κ B stimulation in response to TRAF-6 mediated activation.

Significantly, E57K NEMO mutant did not affect integration of NEMO into IKK (Figure 14B). Moreover, to confirm a correct IKK activation I stimulated stably cells expressing NEMO or E57K NEMO mutant with TNF- α . In both cases a normal I κ B- α degradation was observed (Figure 14B lower panel).

4.6 E57K is defective in TRAF6 binding

Because TRAF-6 has been proposed to act as an E3 ligase for NEMO, I wondered at which step E57K mutation perturbed the IL-1 signaling. As shown in Figure 15, a specific interaction between TRAF-6 and wt NEMO was detected after co-transfecting the two molecules in HEK

293T cells. The presence of NEMO was observed in the Flag-TRAF6 immunoprecipitated extracts. In contrast, by co-transfecting NEMO E57K mutant, a decreased amount of protein was pulled down by TRAF6, indicating that the recognition between NEMO and TRAF-6 was defective, most likely causing the subsequent defect in IL-1 pathway (Figure 15A).

There are a subclass of IP-causing mutation comprises 2 missense mutations and a single aa deletion of NEMO that are located within the first 150 aa of the protein (DK90, D113N and R123W). I decided to investigate their interaction with TRAF6 and I found that they associated equally with TRAF6 (Figure 15B and data not shown). Importantly, the DK90 mutant, showing a strong defect in IKK kinases binding (see below), did not have any defect in TRAF6 interaction. Likewise, as previously discussed, E57K did not affect binding to both IKK related kinases, indicating that separate neighboring sequences are required for binding of TRAF6 and IKK to NEMO.

In parallel, to confirm that the region of NEMO containing E57K mutation provided binding site for TRAF6, a deletion analysis was also carried out using small internal deletions located at the N-terminus of the NEMO protein (see Marienfeld, Palkowitsch et al. 2006 for details). Removing aa 47 to 56 (del5) reduced to some extent TRAF6 binding whereas removing aa 57 to 69 (del6) was very deleterious. In contrast, removing aa 70 to 79 (del7) appeared without any effect (Figure 15C). Importantly, also in this case, the interaction of del6 with IKK2 was unaffected (Marienfeld, Palkowitsch et al. 2006). Collectively, these results strongly suggest that the defect in TRAF6 interaction was not caused by the absence of a small helical domain participating in IKK recognition at the N-terminus of NEMO.

4.7 Mapping the TRAF6 binding site of NEMO

Several truncated forms of TRAF6 were examined for their ability to interact with NEMO (Figure 16A). Like other TRAFs, TRAF6 has a

conserved C-terminus TRAF-C domain, a TRAF-N domain and an N-terminus ring finger (Cao, Xiong et al. 1996).

Removing the first 297 aa of TRAF6, which contain both the ring finger and the five zinc fingers did not affect binding of TRAF6 to NEMO (Fig. 16B, lower panel). In contrast, the interaction was lost deleting C-terminus portion of the TRAFN domain such as in Del330 TRAF6 (Figure 16B, upper panel). Conversely, deleting the TRAF-C domain of TRAF6 did not affect binding of TRAF6 to NEMO (Figure 16B, upper panel) but eliminating N-terminus of the TRAFN domain, such as in DC308 TRAF6, impaired NEMO binding. This suggested that TRAFN domain of TRAF6, which was predicted to have a structure of a coiled coil (CC), might be responsible for TRAF6 interaction with the N-terminus of NEMO. To confirm this hypothesis an internal deletion of TRAF6 only lacking residues 301 to 358 (DCC-TRAF6) was prepared. It exhibited a strong defect in NEMO binding (Figure 16B, lower panel). While all TRAF6 residues present at its interface with NEMO are conserved among species, most are not conserved in TRAF2 that is known to mediate NF- κ B activation in TNF pathway. In fact, the full-length of TRAF2 did not interact with NEMO in the same assay using 293T cells. Taken together, these results clearly indicated that the CC domain of TRAF6 played a key role in mediating direct interaction with NEMO.

4.8 The Lysine 90: the critical residue for IKK complex formation

I decided to further investigate an in frame deletion of a codon (266-269delAGA) leading to a microdeletion of a K-90 (DK90) falling in the CC1 domain of NEMO protein. The DK90 mutation has been found in a patient suffering from a severe form of IP in which also nervous system (brain atrophy, microcephaly, mental retardation, epilepsy and spastic paralysis were observed) and eyes are affected (strabismus and retinal haemorrhage were shown). The mutation was published in 2004 (Fusco,

Bardaro et al. 2004) but its molecular defect was not completely resolved.

To add informations regarding the functional relevance of K90, I complemented MEFs NEMO (-) cells via retroviral infection. I assessed the NF- κ B activation after TNF and IL-1 stimulation. As shown in Figure 17A, DK90 exhibited a strong impairment affecting both the TNF and the IL-1 signaling pathways. Importantly, a correct expression of DK90 NEMO mutant protein was confirmed by western blot analysis (figure 17A).

Later on, since the IKK-binding region of NEMO has recently been confined to residues 47-120 (Marienfeld, Palkowitsch et al. 2006), I investigated the ability of DK90 to associate with IKKs in HEK293T cells.

Cells were transiently co-transfected with DK90 or NEMO expression vector in combinations with either FLAG-IKK2 or HA-IKK1 plasmids. Cell extracts were immunoprecipitated with an anti-FLAG antibody or anti-NEMO and then analyzed by immunoblotting assay with an anti-NEMO or anti-HA respectively (Fig. 17B).

I found that a deletion of a K90 completely abolish the NEMO interaction with IKK1 while strongly reduced its interaction with IKK2 demonstrating a critical role of the K90 residue in NEMO/IKK complex formation.

5. DISCUSSION

Incontinentia Pigmenti (IP) is the first genetic disease associated to NF- κ B alteration. It provides the best insight into the physiological role of the regulatory subunit NEMO in the IKK complex activation. To this respect, the characterization of IP-related NEMO mutants represents an exclusive opportunity to elucidate the molecular mechanism of IKK regulation. In this study, I reported on the molecular characterization of three IP-related NEMO mutation, two are missense mutations, A323P and E57K, and one is an in frame deletion causing the deletion of Lysine 90 (DK90).

A323P is a newly described mutation found in a patient suffering for a severe form of IP. As expected, this substitution caused a severe defect in NF- κ B activation involving several distinct pathways. I found that A323P shown an impaired TRAF6-dependent NEMO ubiquitination, explaining the defects associated to IL-1 and LPS signaling. In addition, by site directed mutagenesis and a deletion analysis of NEMO, I have identified three new lysine residues, located around A323, which are targeted by TRAF6. The critical TRAF-6-dependent ubiquitinated sites on NEMO are required for NF- κ B activation and appear to integrate signaling pathways that are used by a variety of stimuli all using TRAF6 as E3 ligase. It remains uncertain how their modification by ubiquitination influence the IKK activation process, in particular if they provide a primary tag for building up interactions between components regulating IKK activity or represent the final step triggering its catalytic activation..

Regarding the A323P defect in TNF-mediated activation, it is noteworthy to mention that during my characterization of this mutant, three unrelated groups showed the existence of the “sensor” pathway. Upon TNF stimulation, NEMO, through NUB domain, appears to act as a sensor to associate to the ubiquitinated RIP leading to the IKK activation. Point mutations within the NUB domain have been reported to impair recognition of ubiquitinated RIP by NEMO. Since A323P is located in close proximity of NUB, it is likely that impaired NF- κ B activation in response to TNF is caused by a defective recruitment of IKK to TNF-R1 (Ea, Deng et al. 2006;

Li, Kobayashi et al. 2006; Wu, Conze et al. 2006).

Dissecting the molecular defects associated to E57K missense mutation I have discovered a new protein/protein interface that is required for NEMO/TRAF6 interaction.

NEMO E57K mutation was associated to a specific defect in IL-1-mediated NF- κ B activation, resulting from a reduced interaction between E57K NEMO and TRAF6. The sequence involved in this interaction, located at the N-terminus of NEMO, has been shown also to bind IKK1 and 2. Ruche and colleagues have recently demonstrated that the N-terminus part of NEMO (44-111) is formed of distinct alfa-helical subdomains, which not only provide interfaces for heterotypic interaction with IKK1/IKK2 but also allow dimerization of NEMO. Moreover, they have solved the crystal structure of the NEMO/IKK interaction and several critical residues of NEMO, participating either in recognition by IKKs or in NEMO dimerization, have been identified (Rushe, Silvian et al. 2008). In particular, the E57 residue appears to participate in NEMO N-ter dimerization. Thus, I hypothesized that a single modification of this binding interface, like the change of charge resulting from E57K mutation, may specifically perturb the binding of NEMO to TRAF6.

On the TRAF6 side, a new putative function of the TRAF6 CC in NF- κ B activation has emerged. Until now, the role of this domain was quite unclear in contrast to the well-known functions of the ring finger and TRAF-C domains. TRAF6 has been shown to play key roles in NF- κ B-dependent signaling pathways controlling most cellular processes. It therefore represents an attractive target for inhibiting NF- κ B activation when its activation is dysregulated, such as in inflammation, cancer or autoimmunity.

The last mutation I analysed is DK90, an in frame deletion of a codon resulting in a Lysine deletion at position 90. In this case, detailed analysis of NF- κ B activity in response to TNF, IL-1 and LPS has shown a strong defect in all these signaling pathways. I have found that mutant protein completely lost its ability to interact with IKK1 while it retained some capacity to bind IKK2. This difference probably is due to the higher

affinity of IKK2 for NEMO compared with IKK1. Why NEMO has different affinities for IKK1 and IKK2 is still unknown but the answer to this question may provide a clue in understanding the distinct functions of the IKKs.

In summary, this work provides new insights into the role of NEMO *in vivo* and a better understanding of IP at the cellular and molecular levels. Importantly, dissecting specific molecular interactions within the NEMO-mediated activation could suggest new targets for the development of potentially effective therapeutic strategies, not only for this specific pathology but also for more common pathologies resulting from NF- κ B dysfunction.

However, the main question regarding how these series of molecular defects, affecting different signaling pathways, impact on the high variable phenotype displayed by the IP patients remains still unclear. In particular, it is difficult to understand why some mutations generated severe CNS abnormalities. Even if random variations in X-inactivation skewing have been shown to cause extended phenotype heterogeneity in patients carrying the same NEMO rearrangement, it is possible that a discrete pathway participating in CNS development/functioning may be specifically affected by A323P or DK90 mutation. Analyzing NEMO-IP mutation in an *in vivo* system, such as knock-in mice, may be useful to verify this hypothesis.

6. REFERENCES

- Abbott, D. W., Y. Yang, et al. (2007). "Coordinated regulation of Toll-like receptor and NOD2 signaling by K63-linked polyubiquitin chains." Mol Cell Biol **27**(17): 6012-25.
- Agou, F., G. Courtois, et al. (2004). "Inhibition of NF-kappa B activation by peptides targeting NF-kappa B essential modulator (nemo) oligomerization." J Biol Chem **279**(52): 54248-57.
- Aradhya, S., T. Bardaro, et al. (2001). "Multiple pathogenic and benign genomic rearrangements occur at a 35 kb duplication involving the NEMO and LAGE2 genes." Hum Mol Genet **10**(22): 2557-67.
- Aradhya, S., H. Woffendin, et al. (2001). "A recurrent deletion in the ubiquitously expressed NEMO (IKK-gamma) gene accounts for the vast majority of incontinentia pigmenti mutations." Hum Mol Genet **10**(19): 2171-9.
- Bignell, G. R., W. Warren, et al. (2000). "Identification of the familial cylindromatosis tumour-suppressor gene." Nat Genet **25**(2): 160-5.
- Bonizzi, G. and M. Karin (2004). "The two NF-kappaB activation pathways and their role in innate and adaptive immunity." Trends Immunol **25**(6): 280-8.
- Brown, K. D., B. S. Hostager, et al. (2002). "Regulation of TRAF2 signaling by self-induced degradation." J Biol Chem **277**(22): 19433-8.
- Burkly, L., C. Hession, et al. (1995). "Expression of relB is required for the development of thymic medulla and dendritic cells." Nature **373**(6514): 531-6.
- Cao, Z., J. Xiong, et al. (1996). "TRAF6 is a signal transducer for interleukin-1." Nature **383**(6599): 443-6.

- Chen, Z. J., L. Parent, et al. (1996). "Site-specific phosphorylation of IkappaBalpha by a novel ubiquitination-dependent protein kinase activity." Cell **84**(6): 853-62.
- Courtois, G. and T. D. Gilmore (2006). "Mutations in the NF-kappaB signaling pathway: implications for human disease." Oncogene **25**(51): 6831-43.
- Courtois, G., S. T. Whiteside, et al. (1997). "Characterization of a mutant cell line that does not activate NF-kappaB in response to multiple stimuli." Mol Cell Biol **17**(3): 1441-9.
- Deng, L., C. Wang, et al. (2000). "Activation of the IkappaB kinase complex by TRAF6 requires a dimeric ubiquitin-conjugating enzyme complex and a unique polyubiquitin chain." Cell **103**(2): 351-61.
- Doffinger, R., A. Smahi, et al. (2001). "X-linked anhidrotic ectodermal dysplasia with immunodeficiency is caused by impaired NF-kappaB signaling." Nat Genet **27**(3): 277-85.
- Ea, C. K., L. Deng, et al. (2006). "Activation of IKK by TNFalpha requires site-specific ubiquitination of RIP1 and polyubiquitin binding by NEMO." Mol Cell **22**(2): 245-57.
- Fu, D. X., Y. L. Kuo, et al. (2003). "Human T-lymphotropic virus type I tax activates I-kappa B kinase by inhibiting I-kappa B kinase-associated serine/threonine protein phosphatase 2A." J Biol Chem **278**(3): 1487-93.
- Fusco, F., T. Bardaro, et al. (2004). "Molecular analysis of the genetic defect in a large cohort of IP patients and identification of novel NEMO mutations interfering with NF-kappaB activation." Hum Mol Genet **13**(16): 1763-73.

- Fusco, F., M. Paciolla, et al. (2009). "Microdeletion/duplication at the Xq28 IP locus causes a de novo IKBKG/NEMO/IKKgamma exon4_10 deletion in families with Incontinentia Pigmenti." Hum Mutat **30**(9): 1284-91.
- Fusco, F., A. Pescatore, et al. (2008). "Alterations of the IKBKG locus and diseases: an update and a report of 13 novel mutations." Hum Mutat **29**(5): 595-604.
- Geetha, T., J. Jiang, et al. (2005). "Lysine 63 polyubiquitination of the nerve growth factor receptor TrkA directs internalization and signaling." Mol Cell **20**(2): 301-12.
- Gilmore, T. D. (1999). "The Rel/NF-kappaB signal transduction pathway: introduction." Oncogene **18**(49): 6842-4.
- Gilmore, T. D. (2006). "Introduction to NF-kappaB: players, pathways, perspectives." Oncogene **25**(51): 6680-4.
- Hacker, H. and M. Karin (2006). "Regulation and function of IKK and IKK-related kinases." Sci STKE **2006**(357): re13.
- Hadj-Rabia, S., D. Froidevaux, et al. (2003). "Clinical study of 40 cases of incontinentia pigmenti." Arch Dermatol **139**(9): 1163-70.
- Harhaj, E. W., L. Good, et al. (2000). "Somatic mutagenesis studies of NF-kappa B signaling in human T cells: evidence for an essential role of IKK gamma in NF-kappa B activation by T-cell costimulatory signals and HTLV-I Tax protein." Oncogene **19**(11): 1448-56.
- Hayden, M. S. and S. Ghosh (2008). "Shared principles in NF-kappaB signaling." Cell **132**(3): 344-62.
- Hicke, L., H. L. Schubert, et al. (2005). "Ubiquitin-binding domains." Nat Rev

Mol Cell Biol **6**(8): 610-21.

Hoffmann, A., T. H. Leung, et al. (2003). "Genetic analysis of NF-kappaB/Rel transcription factors defines functional specificities." Embo J **22**(20): 5530-9.

Hu, Y., V. Baud, et al. (2001). "IKKalpha controls formation of the epidermis independently of NF-kappaB." Nature **410**(6829): 710-4.

Ikeda, F. and I. Dikic (2008). "Atypical ubiquitin chains: new molecular signals. 'Protein Modifications: Beyond the Usual Suspects' review series." EMBO Rep **9**(6): 536-42.

Inohara, N., T. Koseki, et al. (2000). "An induced proximity model for NF-kappa B activation in the Nod1/RICK and RIP signaling pathways." J Biol Chem **275**(36): 27823-31.

Ishitani, T., G. Takaesu, et al. (2003). "Role of the TAB2-related protein TAB3 in IL-1 and TNF signaling." Embo J **22**(23): 6277-88.

Karin, M. and Y. Ben-Neriah (2000). "Phosphorylation meets ubiquitination: the control of NF-[kappa]B activity." Annu Rev Immunol **18**: 621-63.

Kenwrick, S., H. Woffendin, et al. (2001). "Survival of male patients with incontinentia pigmenti carrying a lethal mutation can be explained by somatic mosaicism or Klinefelter syndrome." Am J Hum Genet **69**(6): 1210-7.

Klemm, S., S. Zimmermann, et al. (2007). "Bcl10 and Malt1 control lysophosphatidic acid-induced NF-kappaB activation and cytokine production." Proc Natl Acad Sci U S A **104**(1): 134-8.

Kontgen, F., R. J. Grumont, et al. (1995). "Mice lacking the c-rel proto-oncogene exhibit defects in lymphocyte proliferation, humoral

immunity, and interleukin-2 expression." Genes Dev **9**(16): 1965-77.

Kovalenko, A., C. Chable-Bessia, et al. (2003). "The tumour suppressor CYLD negatively regulates NF-kappaB signalling by deubiquitination." Nature **424**(6950): 801-5.

Lamothe, B., A. Besse, et al. (2007). "Site-specific Lys-63-linked tumor necrosis factor receptor-associated factor 6 auto-ubiquitination is a critical determinant of I kappa B kinase activation." J Biol Chem **282**(6): 4102-12.

Lamothe, B., A. D. Campos, et al. (2008). "The RING domain and first zinc finger of TRAF6 coordinate signaling by interleukin-1, lipopolysaccharide, and RANKL." J Biol Chem **283**(36): 24871-80.

Landy, S. J. and D. Donnai (1993). "Incontinentia pigmenti (Bloch-Sulzberger syndrome)." J Med Genet **30**(1): 53-9.

Li, H., M. Kobayashi, et al. (2006). "Ubiquitination of RIP is required for tumor necrosis factor alpha-induced NF-kappaB activation." J Biol Chem **281**(19): 13636-43.

Li, Z. W., W. Chu, et al. (1999). "The IKKbeta subunit of IkappaB kinase (IKK) is essential for nuclear factor kappaB activation and prevention of apoptosis." J Exp Med **189**(11): 1839-45.

Marienfeld, R. B., L. Palkowitsch, et al. (2006). "Dimerization of the I kappa B kinase-binding domain of NEMO is required for tumor necrosis factor alpha-induced NF-kappa B activity." Mol Cell Biol **26**(24): 9209-19.

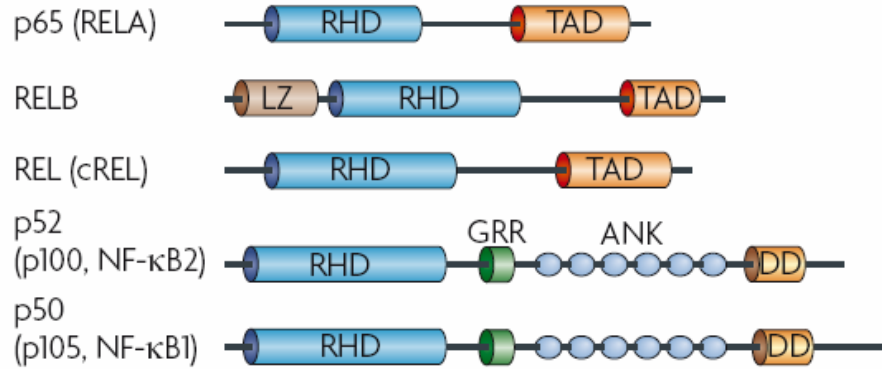
Mukhopadhyay, D. and H. Riezman (2007). "Proteasome-independent functions of ubiquitin in endocytosis and signaling." Science **315**(5809): 201-5.

- Newton, K., M. L. Matsumoto, et al. (2008). "Ubiquitin chain editing revealed by polyubiquitin linkage-specific antibodies." Cell **134**(4): 668-78.
- Palkowitsch, L., J. Leidner, et al. (2008). "Phosphorylation of serine 68 in the IkappaB kinase (IKK)-binding domain of NEMO interferes with the structure of the IKK complex and tumor necrosis factor-alpha-induced NF-kappaB activity." J Biol Chem **283**(1): 76-86.
- Park, Y. C., V. Burkitt, et al. (1999). "Structural basis for self-association and receptor recognition of human TRAF2." Nature **398**(6727): 533-8.
- Pickart, C. M. (2004). "Back to the future with ubiquitin." Cell **116**(2): 181-90.
- Pineda, G., C. K. Ea, et al. (2007). "Ubiquitination and TRAF signaling." Adv Exp Med Biol **597**: 80-92.
- Poyet, J. L., S. M. Srinivasula, et al. (2000). "Activation of the Ikappa B kinases by RIP via IKKgamma /NEMO-mediated oligomerization." J Biol Chem **275**(48): 37966-77.
- Rushe, M., L. Silvan, et al. (2008). "Structure of a NEMO/IKK-associating domain reveals architecture of the interaction site." Structure **16**(5): 798-808.
- Schmidt-Supprian, M., W. Bloch, et al. (2000). "NEMO/IKK gamma-deficient mice model incontinentia pigmenti." Mol Cell **5**(6): 981-92.
- Sebban, H. and G. Courtois (2006). "NF-kappaB and inflammation in genetic disease." Biochem Pharmacol **72**(9): 1153-60.
- Sebban, H., S. Yamaoka, et al. (2006). "Posttranslational modifications of NEMO and its partners in NF-kappaB signaling." Trends Cell Biol **16**(11): 569-77.

- Sen, R. and D. Baltimore (1986). "Multiple nuclear factors interact with the immunoglobulin enhancer sequences." Cell **46**(5): 705-16.
- Skaug, B., X. Jiang, et al. (2009). "The role of ubiquitin in NF-kappaB regulatory pathways." Annu Rev Biochem **78**: 769-96.
- Smahi, A., G. Courtois, et al. (2000). "Genomic rearrangement in NEMO impairs NF-kappaB activation and is a cause of incontinentia pigmenti. The International Incontinentia Pigmenti (IP) Consortium." Nature **405**(6785): 466-72.
- Sun, L., L. Deng, et al. (2004). "The TRAF6 ubiquitin ligase and TAK1 kinase mediate IKK activation by BCL10 and MALT1 in T lymphocytes." Mol Cell **14**(3): 289-301.
- Tang, E. D., C. Y. Wang, et al. (2003). "A role for NF-kappaB essential modifier/IkappaB kinase-gamma (NEMO/IKKgamma) ubiquitination in the activation of the IkappaB kinase complex by tumor necrosis factor-alpha." J Biol Chem **278**(39): 37297-305.
- Thrower, J. S., L. Hoffman, et al. (2000). "Recognition of the polyubiquitin proteolytic signal." Embo J **19**(1): 94-102.
- Wagner, S., I. Carpentier, et al. (2008). "Ubiquitin binding mediates the NF-kappaB inhibitory potential of ABIN proteins." Oncogene **27**(26): 3739-45.
- Wang, C., L. Deng, et al. (2001). "TAK1 is a ubiquitin-dependent kinase of MKK and IKK." Nature **412**(6844): 346-51.
- Weih, F., D. Carrasco, et al. (1995). "Multiorgan inflammation and hematopoietic abnormalities in mice with a targeted disruption of RelB, a member of the NF-kappa B/Rel family." Cell **80**(2): 331-40.

- Wu, C. J., D. B. Conze, et al. (2006). "Sensing of Lys 63-linked polyubiquitination by NEMO is a key event in NF-kappaB activation [corrected]." Nat Cell Biol **8**(4): 398-406.
- Xiao, G., A. Fong, et al. (2004). "Induction of p100 processing by NF-kappaB-inducing kinase involves docking IkappaB kinase alpha (IKKalpha) to p100 and IKKalpha-mediated phosphorylation." J Biol Chem **279**(29): 30099-105.
- Yang, C., W. Zhou, et al. (2006). "Negative regulation of the E3 ubiquitin ligase itch via Fyn-mediated tyrosine phosphorylation." Mol Cell **21**(1): 135-41.
- Zhang, S. Q., A. Kovalenko, et al. (2000). "Recruitment of the IKK signalosome to the p55 TNF receptor: RIP and A20 bind to NEMO (IKKgamma) upon receptor stimulation." Immunity **12**(3): 301-11.
- Zonana, J., M. E. Elder, et al. (2000). "A novel X-linked disorder of immune deficiency and hypohidrotic ectodermal dysplasia is allelic to incontinentia pigmenti and due to mutations in IKK-gamma (NEMO)." Am J Hum Genet **67**(6): 1555-62.

NF- κ B family



I κ B family

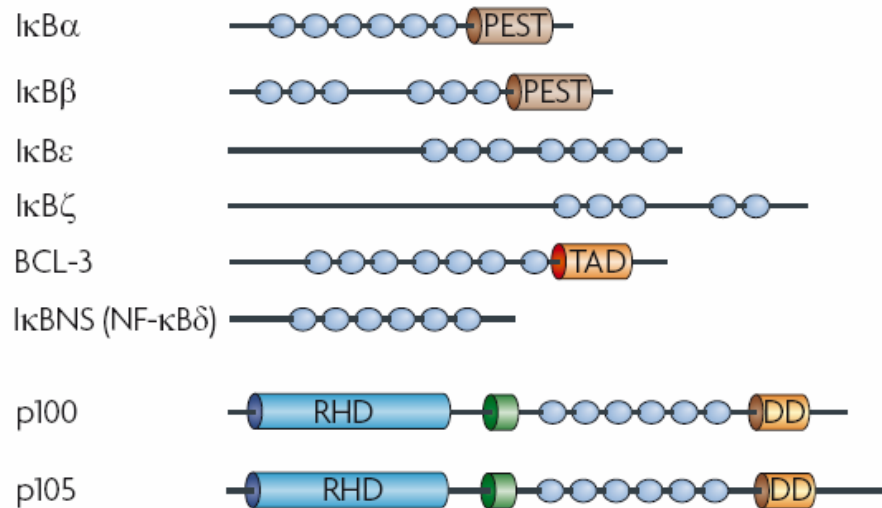


Figure 1
Members of NF- κ B and I κ B protein families

The domains that typify each protein family are indicated, and alternative nomenclatures are provided in brackets. The precursor proteins p100 and p105 function as both inhibitor of nuclear factor- κ B (NF- κ B) proteins and, when processed by the proteasome, NF- κ B family members. ANK, ankyrin-repeat; BCL-3, B-cell lymphoma 3; CC, coiled-coil; DD, death domain; GRR, glycine-rich region; HLH, helix-loop-helix;

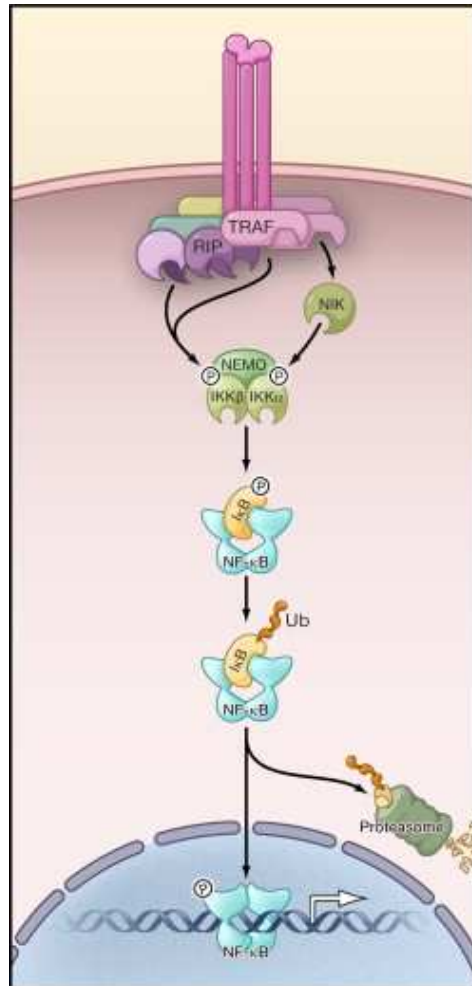


Figure 2
NF- κ B Signaling Pathways

Following receptor ligation and recruitment of receptor proximal adaptor proteins, signaling to IKK proceeds through TRAF/RIP complexes, generally in conjunction with TAK1, leading to canonical NF- κ B signaling, or through TRAFs and NIK leading to the noncanonical NF- κ B pathway. IKK activation results in I κ B phosphorylation and degradation in the canonical pathway or p100 processing to p52 in the noncanonical pathway. Phosphorylated NF- κ B dimers bind to κ B DNA elements and induce transcription of target genes.

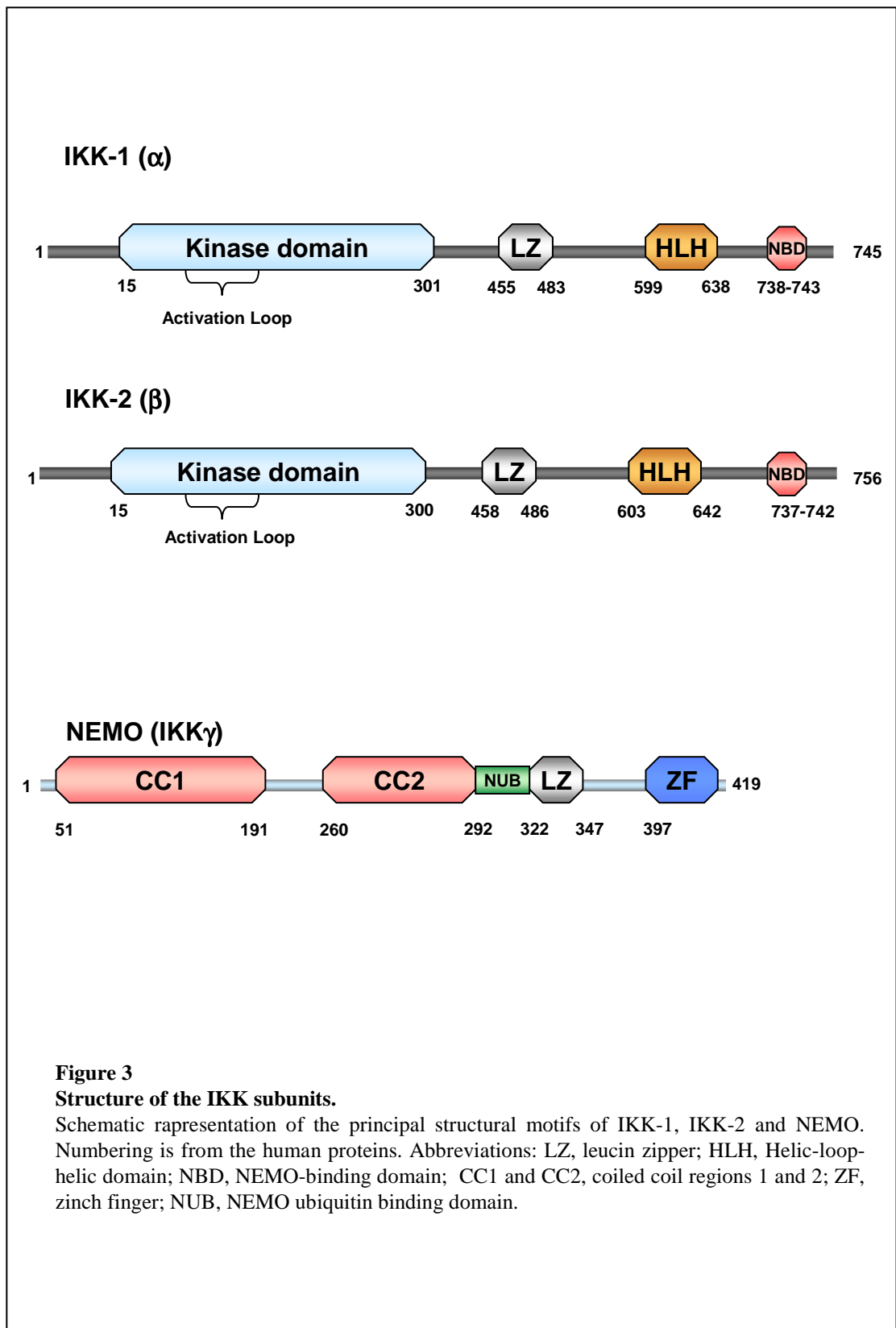
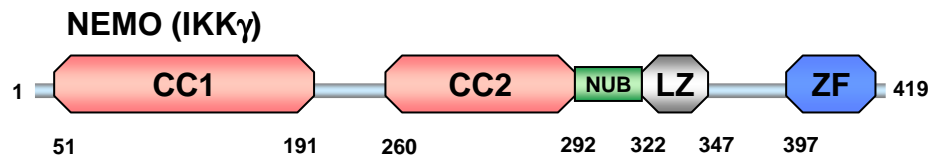


Figure 3
Structure of the IKK subunits.

Schematic representation of the principal structural motifs of IKK-1, IKK-2 and NEMO. Numbering is from the human proteins. Abbreviations: LZ, leucin zipper; HLH, Helic-loop-helic domain; NBD, NEMO-binding domain; CC1 and CC2, coiled coil regions 1 and 2; ZF, zinch finger; NUB, NEMO ubiquitin binding domain.

Table 1
The NEMO interactome.



Protein name ^b	Pathway or function	Part of the NEMO sequence bound
ABIN-1	TNF signaling pathway; negative regulator of IKK	51–100
A20	Negative regulator of RIP; K63 deubiquitinase; K48 E3 ligase	n.d.
CARDINAL	Inhibitor of IKK	n.d.
CARMA-1/3	TCR and BCR signaling pathways; scaffold	51–100
c-IAP-1	TNF signaling pathway; E3 ligase	n.d.
CIKS/Act-1	CD40 pathway; adaptor	50–100
v-CLAP	EHV-2-derived; Bcl10-like	200–300
CYLD	Negative regulator of IKK; K63 deubiquitinase	388–393
ELKS	Subunit of IKK; κ Bs recruitment	n.d.
E3-14.7K	Adenovirus-derived; activator of IKK	397–419
p22-FLIP	Inhibitor of death receptor-mediated apoptosis	n.d.
v-FLIP	KSHV-derived; activator of IKK	150–272
HIF-2a ^c	Hypoxia-inducible factor	n.d.
Hsp70	Heat shock response; inhibitor of IKK	250–320
Htt	Mutant form of Huntingtin; neurotoxicity	n.d.
IKK-1	Subunit of IKK; phosphorylation of κ Bs and p100	60–119
IKK-2	Subunit of IKK; phosphorylation of κ Bs	60–119
Myo1c ^c	Unconventional myosin I; insulin signaling	n.d.
PP2A	TNF signaling pathway; phosphatase	121–179
RICK	TLR4, TCR, IL-12, IL-18 and Nod2 signaling pathways; adaptor	n.d.
RIP	TNF and TLR signaling pathways; adaptor	134–218
TANK	TNF signaling pathway; adaptor	200–250
Tax	HTLV-1-derived; activator of IKK	262–315
TRUSS	TNF signaling pathway; scaffold	n.d.
ZNF216	RIP-, TRAF-6- and A20-binding protein	n.d.

Sebban, Yamaoka et al. 2006

A)

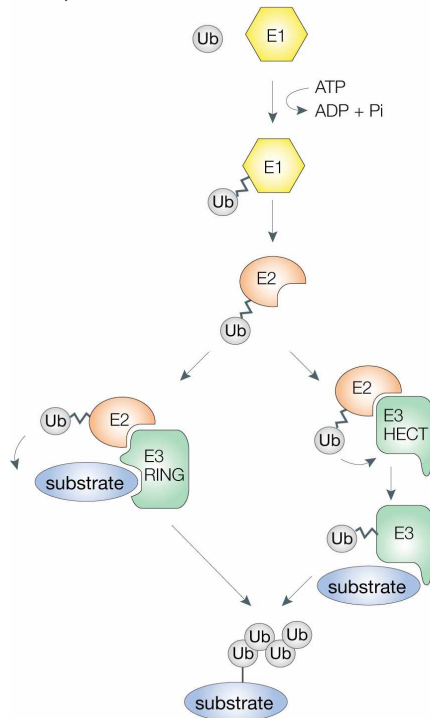


Figure 4

The ubiquitin pathway. A) Schematic representation of the ubiquitination process. A hierarchical set of three types of enzyme is required for substrate ubiquitination: ubiquitin-activating (E1), ubiquitin-conjugating (E2) and ubiquitin-protein ligase (E3) enzymes. The two major classes of E3 ligases are depicted. B) Schematic representation of the different Ub modifications with their functional roles. The question mark indicates that the functions of branched chains are largely unknown.

B)

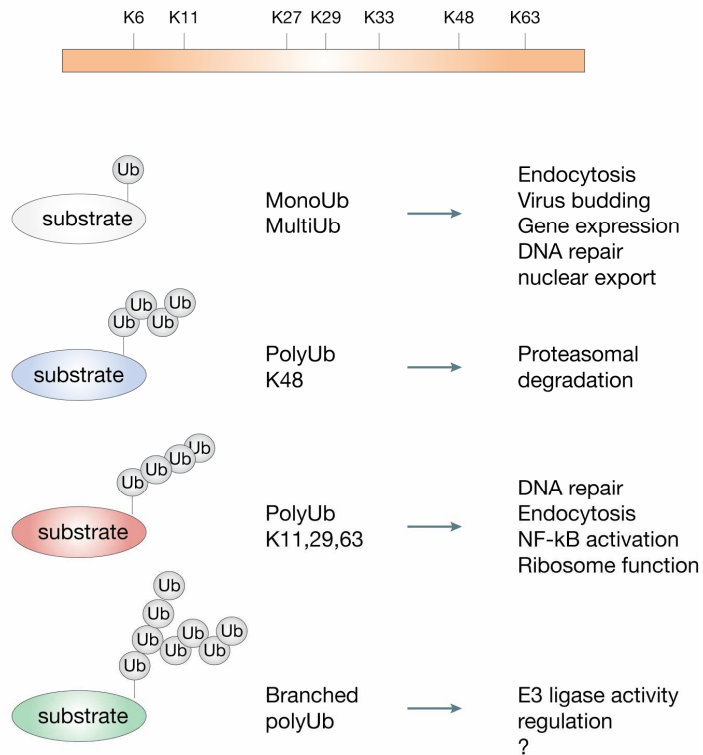


Table 2
Representative proteins involved in ubiquitin-mediated regulation of IKK

Protein category	Protein name or family	Domain architecture
E2	UBC5/UBC13	UBC
E3	TRAF	RING ZnF CC TRAF
	TRIM25	RING B box/CCD SPRY
	c-IAP	BIR CARD RING
	ITCH	C2 WW HECT
Ub target	TRAF	See above
	RIP1	Kinase CC DD
	RIP2	Kinase CARD
	RIG-I	CARD Helicase
	NEMO	IKK binding CC1 CC2 LZ ZnF UBD
	IRAK1	DD Kinase
E3 regulator/ Ub target	MALT1	DD IgG Caspase like
	BCL10	CARD
Ub receptor	NEMO	See above
	TAB2/3	CUE ZnF
Deubiquitination enzyme (DUB)	CYLD	CAP-GLY USP
	A20	OTU ZnF
	DUBA	OTU UIM

Skaug, Jiang et al. 2009

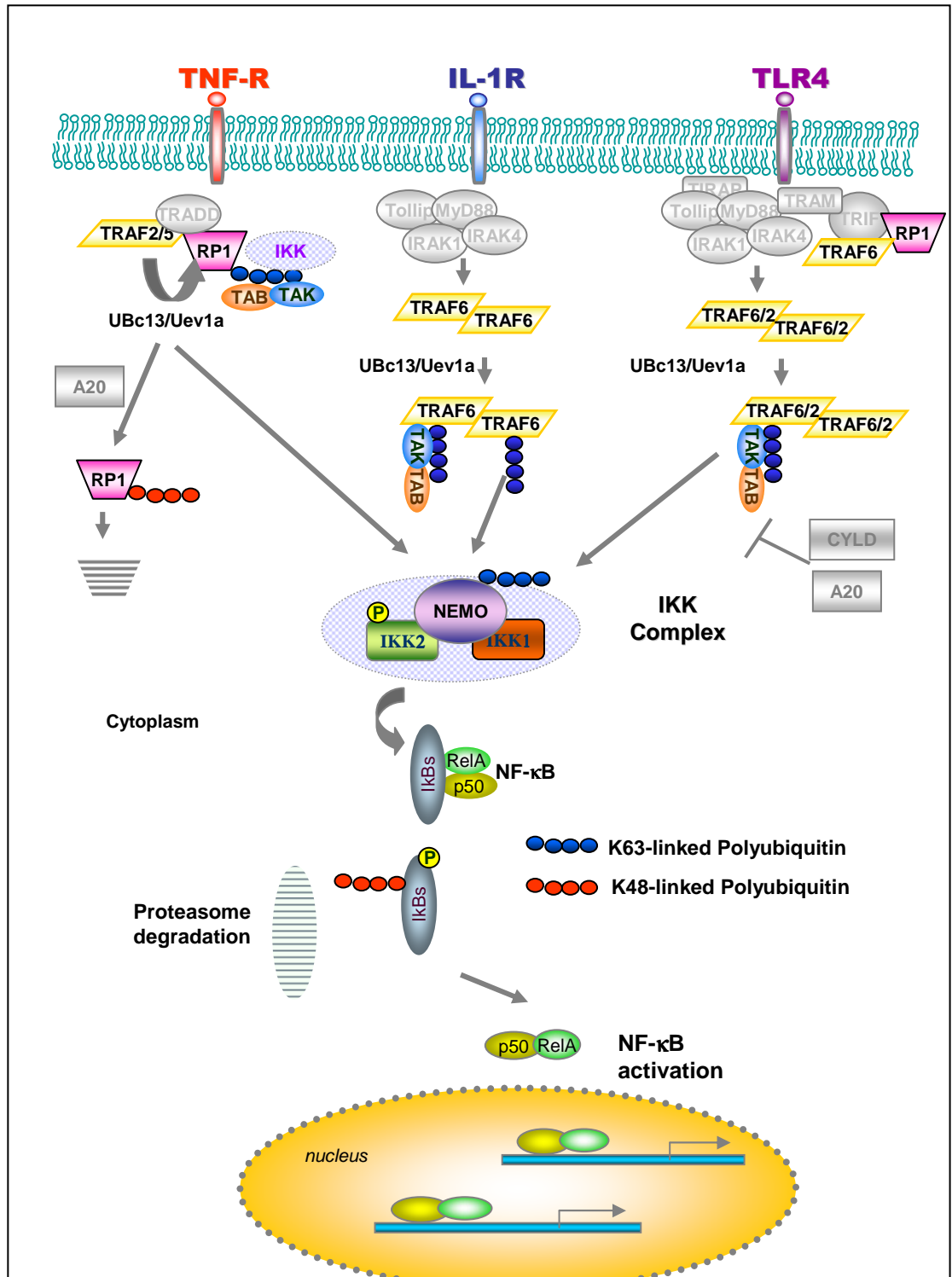


Figure 5
Role of ubiquitin and IKK complex in coordinating NF-κB activation.
 The major molecules involved in IL-1, TNF and TLR4 signaling pathways and participating in NF-κB regulation are presented.

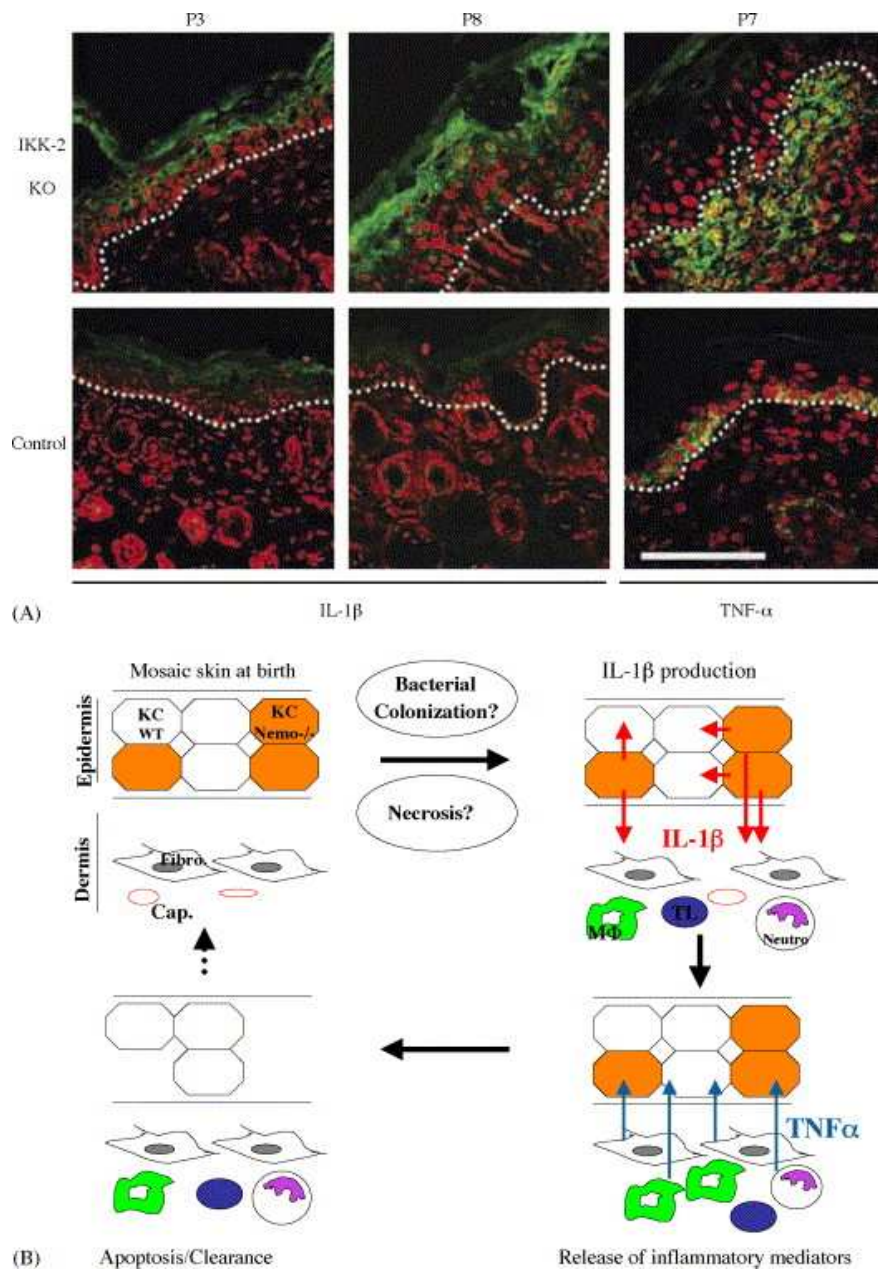


Figure 6

Molecular and cellular events associated with IP dermatosis.

(A) Immunohistochemistry analysis of *IKK-2* skin K.O. mice. IL-1 β and TNF- α expression is shown at post-natal days 3 (P3), 7 (P7) and 8 (P8). The dotted line indicates the epidermis/dermis boundary. Ct: wild-type mouse, mt: *IKK-2* skin K.O. mouse. (B) A putative model of IP dermatosis. See text for more details. KC: keratinocyte; Fibro: fibroblast; Cap.: capillary vessel; M Φ : macrophage; TL: T lymphocyte; Neutro: neutrophil granulocyte.

Table 3
NEMO (also called IKBKG) mutations accounting for IP and EDA-ID.

Number	change ^a NM_003639.3	Amino acid change ^b NP_003630.1	Exon/ intron	Mutation type	Clinical diagnosis	References	Inheritance	phenotype score [*]
1	c.111dupC ^d	p.Met38HisfsX12	Exon 2	Frameshift	EDA-ID	Niehues et al. [2004]	Familial	ND
2	c.117_127 dup	p.Ser43CysfsX76 ^e	Exon 2	Frameshift	IP	Smahi et al. [2000]	Familial	1
3	c.133C>T ^{c,ah}	p.Gln45X ^{ah}	Exon 2	Nonsense	IP	This report	2 familial cases	1
4	c.169G>A	p.Glu57Lys	Exon 2	Missense	IP	Aradhya et al. [2001c]	Familial	1
5	c.184 C > T ^{c,ah}	p.Arg62X ^{ah}	Exon 2	Nonsense	IP	This report; Smahi et al. [2000]	2 familial cases and 1 sporadic case	2
6	c.214delC	p.Leu72CysfsX43	Exon 3	Frameshift	IP	Aradhya et al. [2001c]	ND	1
7	c.220delG	p.Glu74SerfsX41 ^f	Exon 3	Frameshift	IP	Aradhya et al. [2001c]	ND	1
8	c.229delG ^{ah}	p.Glu77 ArgfsX38 ^{ah}	Exon 3	Frameshift	IP	This report	Sporadic	1
9	c.239T>C	p.Leu80P ^{ro}	Exon 3	Missense	EDA-ID	Ku et al. [2005]	Familial	ND
10	c.256C>T ^{ah}	p.Gln86X ^{ah}	Exon 3	Nonsense	IP	This report	Familial	4
11	c.266_268del ^g	p.Lys90del	Exon 3	In-frame deletion	IP	Fusco et al. [2004]	Sporadic	8
12	c.292C>T	p.Gln98X	Exon 3	Nonsense	IP	Aradhya et al. [2001c]	ND	1
13	c.337G>A ^{c,ah}	p.Asp113Asn ^{ah}	Exon 3	Missense	IP	This report; Fusco et al. [2004]	3 sporadic cases	1
14	c.367 C>T	p.Arg123 Trp	Exon 3	Missense	IP	Fusco et al. [2004]	Familial	1
15	c.399+1G>C	NA	Intron 3	Splice site	IP	Aradhya et al. [2001c]	ND	2
16	c.454delG ^{ah}	p.Glu152 SerfsX129 ^{ah}	Exon 4	Frameshift	IP	This report	Familial	3
17	c.458T>G	p.Leu153Arg	Exon 4	Missense	EDA-ID	Orange et al. [2002]	Familial	ND
18	c.515_516insC ^{ah}	p.Arg173 SerfsX15 ^{ah}	Exon 4	Frameshift	IP	This report	Familial	1
19	c.516delT	p.Arg173 GlyfsX108 ^{ah}	Exon 4	Frameshift	IP	Aradhya et al. [2001c]	ND	1
20	c.517C>G ⁱ	p.Arg173 Gly	Exon 4	Missense	EDA-ID	Ku et al. [2007]	Familial	ND
21	c.518+2T>A	NA	Intron 4	Splice site	IP	Aradhya et al. [2001c]	ND	1
22	c.523dupC ⁱ	p.Arg175 ProfsX13 ⁱ	Exon 5	Frameshift	IP	Aradhya et al. [2001c]	ND	1
23	c.524 G>C	p.Arg175 Pro	Exon 5	Missense	EDA-ID	Doffinger et al. [2001]	Familial	ND
24	c.551_588del	p.Leu184 ArgfsX57 ^m	Exon 5	Frameshift	IP	Aradhya et al. [2001c]	ND	1
25	c.570delG	p.Leu191CysfsX90 ⁿ	Exon 5	Frameshift	IP	Aradhya et al. [2001c]	ND	1
26	c.638_642dup	p.Met215 SerfsX68 ^o	Exon 5	Frameshift	IP	Aradhya et al. [2001c]	ND	1
27	c.639_645del	p.Arg214 SerfsX65 ^p	Exon 5	Frameshift	IP	Aradhya et al. [2001c]	ND	1
28	c.662C>A ^{ah}	p.Ser221X ^{ah}	Exon 5	Nonsense	IP	This report	ND	1
29	c.680T>C	p.Leu227 Pro	Exon 6	Missense	EDA-ID	Doffinger et al. [2001]	Familial	ND
30	c.706C>T ^c	p.Gln236X	Exon 6	Nonsense	IP	Aradhya et al. [2001c]	2 sporadic cases	1
31	c.715C>T	p.Gln239X	Exon 6	Nonsense	IP	Fusco et al. [2004]	Sporadic	2
32	c.723C>G	p.Tyr241X	Exon 6	Nonsense	IP	Aradhya et al. [2001c]	ND	1
33	c.766C>T ^{ah}	p.Arg256X ^{ah}	Exon 6	Nonsense	IP	This report	Familial	2
34	c.768+5G>A	NA	Intron 6	Splice site	EDA-ID	Orstavik et al. [2006]	Familial	ND
35	c.792dupA	p.Gln265 ThrfsX19 ^q	Exon 7	Frameshift	IP	Martinez-Pomar et al. [2005]	Sporadic	1
36	c.811_828del	NA	Exon 7	InFrame deletion	EDA-ID	Ku et al. [2005]	Familial	ND
37	c.863C>G	p.Ala288 Gly	Exon 7	Missense	EDA-ID	Doffinger et al. [2001]	Familial	ND
38	c.868C>T	p.Gln290X	Exon 7	Nonsense	IP	Aradhya et al. [2001c]	ND	1
39	c.896delC	p.Pro299 ArgfsX3 ^r	Exon 7	Frameshift	IP	Aradhya et al. [2001c]	ND	1
40	c.931G>A	p.Asp311Asn	Exon 8	Missense	EDA-ID	Doffinger et al. [2001]	Familial	ND
41	c.944A>C	p.Glu315 Ala	Exon 8	Missense	AMCBX1	Filipe-Santos et al. [2006]	Familial	ND
42	c.943dupG ^s	p.Glu315 GlyfsX80	Exon 8	Frameshift	IP	Fusco et al. [2004]	Familial	4
43	c.956G>A ^c	p.Arg319Gln	Exon 8	Missense	AMCBX1	Filipe-Santos et al. [2006]	2 familial cases	ND
44	c.967 G>C ^{ah}	p.Ala323 Pro ^{ah}	Exon 8	Missense	IP	Sebban-Benin et al. [2007]	Sporadic	7
45	c.1056-1G>A	NA	Intron 8	Splice site	EDA-ID	Orange et al. [2004]	Sporadic	ND
46	c.1078delC ^t	p.His360 MetfsX91	Exon 9	Frameshift	IP	Fusco et al. [2004]	Sporadic	6
47	c.110delC ^{ah}	p.Ala371 Profs*80 ^{ah}	Exon 9	Frameshift	IP	This report	ND	1
48	c.110dupC ^{c,ah}	p.Ala371 ArgfsX24	Exon 9	Frameshift	IP, EDA-ID	Smahi et al. [2000]	2 familial cases	1
49	c.1115dupC ^{c,ah}	p.Ala373 CysfsX22 ^{ah}	Exon 9	Frameshift	IP	This report	2 familial cases	3
50	c.1116delT ^v	p.Ala373 ProfsX78 ^v	Exon 9	Frameshift	IP	Fusco et al. [2004]	Sporadic	5
51	c.1127_1131del ^{ah}	p.Ser377 ProfsX16 ^{ah}	Exon 10	Frameshift	IP	This report	Familial	1
52	c.1136_1137del ^{ah}	p.Leu379 ArgfsX15 ^{ah}	Exon 10	Frameshift	IP	This report	Sporadic	4
53	c.1150C>T	p.Gln384X	Exon 10	Nonsense	IP	Fusco et al. [2004]	Sporadic	3
54	c.1163_1175 del	p.Pro388 HisfsX59 ^{ah}	Exon 10	Frameshift	IP	Aradhya et al. [2001b,c]	Familial	1
55	c.1166_1178dup	p.Asp394 ArgfsX5 ^{ac}	Exon 10	Frameshift	IP	Aradhya et al. [2001b]	Familial	1
56	c.1167delC ^{c,ah}	p.Glu390 ArgfsX61 ^{z,ah}	Exon 10	Frameshift	IP	This report; Aradhya et al. [2001b,c]	3 familial and 1 sporadic case	1
57	c.1167dupC ^{c,ad}	p.Glu390 ArgfsX5	Exon 10	Frameshift	IP, EDA-ID	Zonana et al. [2000]	3 familial cases	ND
58	c.1171G>T	p.Glu391X	Exon 10	Nonsense	EDA-ID	Zonana et al. [2000]	Familial	ND
59	c.1183_1184del ^{ah}	p.Phe395 LeufsX11 ^{ah}	Exon 10	Frameshift	IP, EDA-ID	This report	Familial	ND
60	c.1201C>T	p.Gln401X	Exon 10	Nonsense	EDA-ID	Filipe-Santos et al. [2006]	ND	ND
61	c.1207C>T	p.Gln403 X	Exon 10	Nonsense	EDA-ID	Orange et al. [2002]	Sporadic	ND
62	c.1217A>T	p.Asp406Val	Exon 10	Missense	EDA-ID	Jain et al. [2001]	Sporadic	ND
63	c.1219dupA ^{ae}	p.Met407 AsnfsX13	Exon 10	Frameshift	EDA-ID	Doffinger et al. [2001]	Familial	ND
64	c.1219A>G	p.Met407Val	Exon 10	Missense	EDA-ID	Smahi et al. [2000]	Familial	ND
65	c.1244dupT ^{ah}	p.Met415 HisfsX5 ^{ah}	Exon 10	Frameshift	EDA-ID	This report	ND	ND
66	c.1249T>C ^c	p.Cys417 Arg	Exon 10	Missense	EDA-ID	Zonana et al. [2000]	3 familial cases	ND
67	c.1250G>T	p.Cys417 Phe	Exon 10	Missense	EDA-ID	Doffinger et al. [2001]	Familial	ND
68	c.1250G>A	p.Cys417 Tyr	Exon 10	Missense	EDA-ID	Orange et al. [2004]	Familial	ND
69	c.1259A>G ^c	p.X420 TrpextX27	Exon 10	Nonstop	IP, OL-EDA-ID	Smahi et al. [2000]	2 familial cases	ND
70	c.399-?_1260+?del ^{c,ad}	NA	—	—	IP	Smahi et al. [2000]	ND	1
71	c.399+850_674dup ^{ag}	NA	—	—	EDA-ID	Nishikomori et al. [2004]	Familial	ND

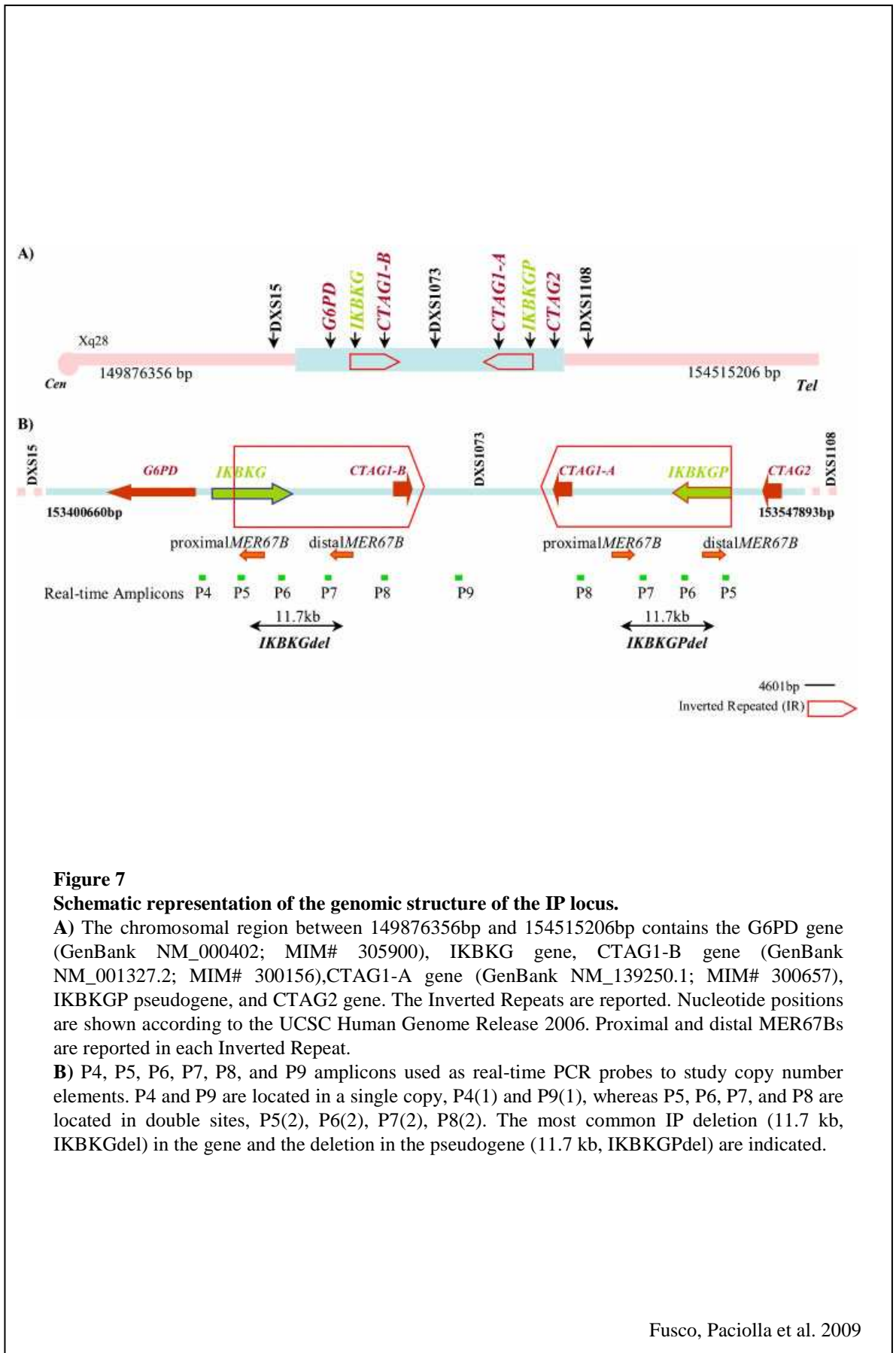
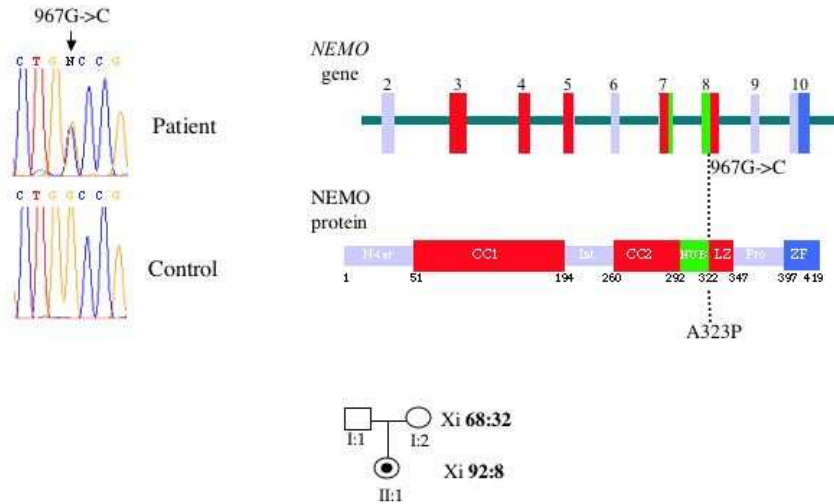


Figure 7
Schematic representation of the genomic structure of the IP locus.

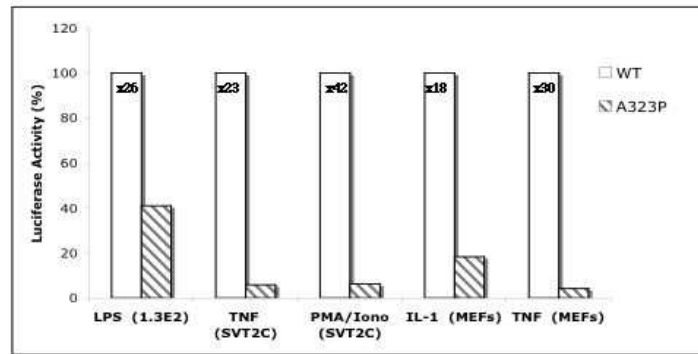
A) The chromosomal region between 149876356bp and 154515206bp contains the *G6PD* gene (GenBank NM_000402; MIM# 305900), *IKBKG* gene, *CTAG1-B* gene (GenBank NM_001327.2; MIM# 300156), *CTAG1-A* gene (GenBank NM_139250.1; MIM# 300657), *IKBKGP* pseudogene, and *CTAG2* gene. The Inverted Repeats are reported. Nucleotide positions are shown according to the UCSC Human Genome Release 2006. Proximal and distal *MER67B*s are reported in each Inverted Repeat.

B) P4, P5, P6, P7, P8, and P9 amplicons used as real-time PCR probes to study copy number elements. P4 and P9 are located in a single copy, P4(1) and P9(1), whereas P5, P6, P7, and P8 are located in double sites, P5(2), P6(2), P7(2), P8(2). The most common IP deletion (11.7 kb, *IKBKGdel*) in the gene and the deletion in the pseudogene (11.7 kb, *IKBKGPdel*) are indicated.

A)



B)



C)

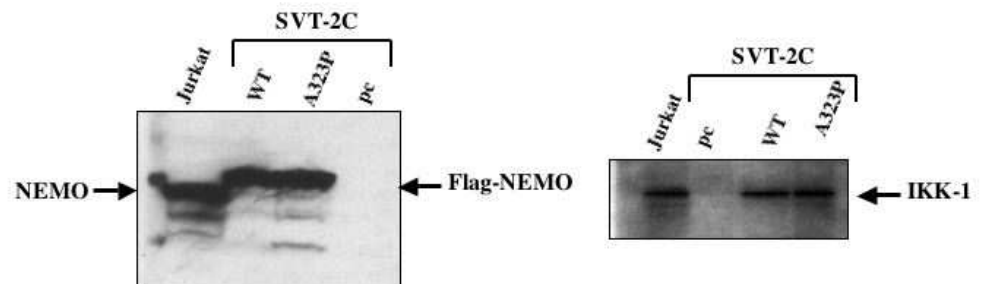


Figure 8.

Identification of a missense mutation of *NEMO* causing a severe form of IP.

A) Sequence analysis and skewed X-inactivation resulting from G967C mutation. The X-inactivation status of the proband (II:1) and her mother (I:2) is indicated in percentage.

B) Phenotype of A323P mutation. Defective response of A323P NEMO mutant to TNF, IL-1, LPS and PMA/ionomycin. Luciferase assays, using IgκB-Luc as a reporter plasmid, were carried out after complementing NEMO^{-/-} cells (SVT-2C, 1.3E2 and MEFs Nemo^{-/-}) with an expression vector encoding either wt or A323P NEMO.

C) Stability of A323P mutant. cells extracts derived from Jurkat or SVT-2C stably expressing NEMO, A323P NEMO or empty vector were analyzed by immunoblotting, using an anti-NEMO (left panel). The same extracts as in were immunoprecipitated with anti-NEMO and analyzed with an anti-IKK-1 (right panel).

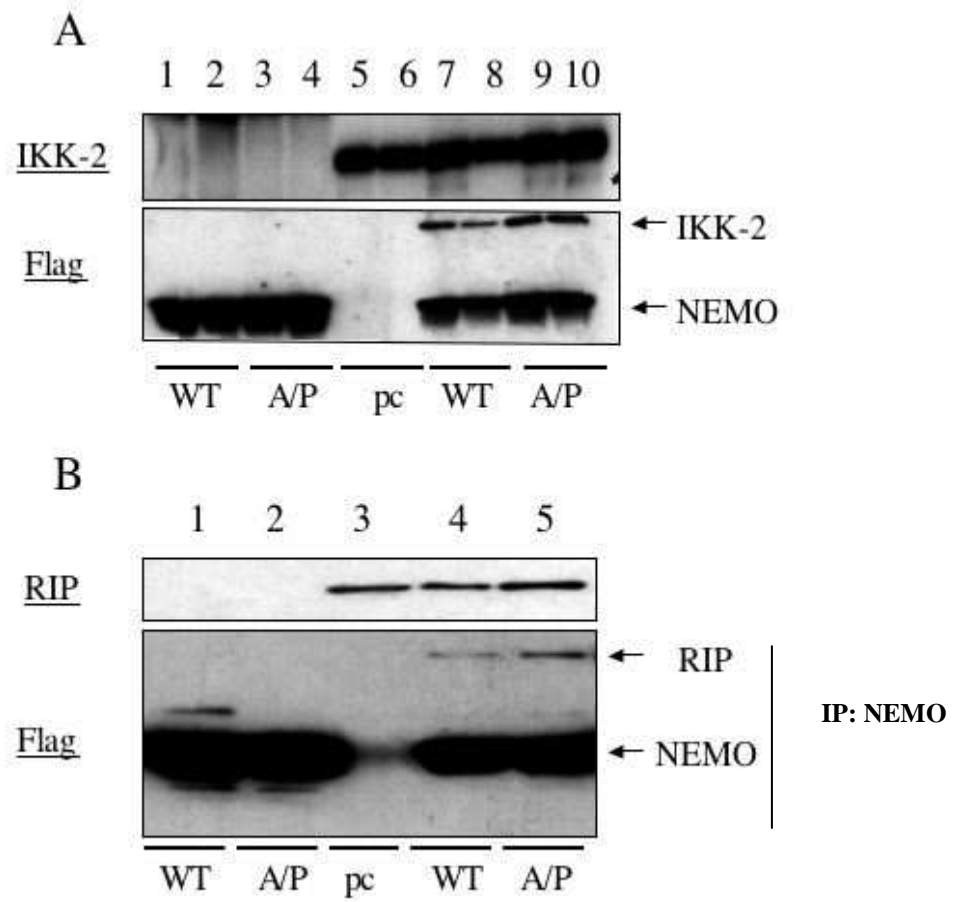


Figure 9

A323P NEMO retained the ability to interact with IKK2 and RIP.

A) HEK 293T cells transiently transfected with Flag-NEMO or Flag-A323P NEMO in combination with Flag-IKK2. The extracts were subjected to anti-NEMO immunoprecipitation. The coimmunoprecipitated IKK2 was analysed by immunoblotting using an anti-Flag.

B) Interaction between A323P NEMO and RIP was analyzed as in A).

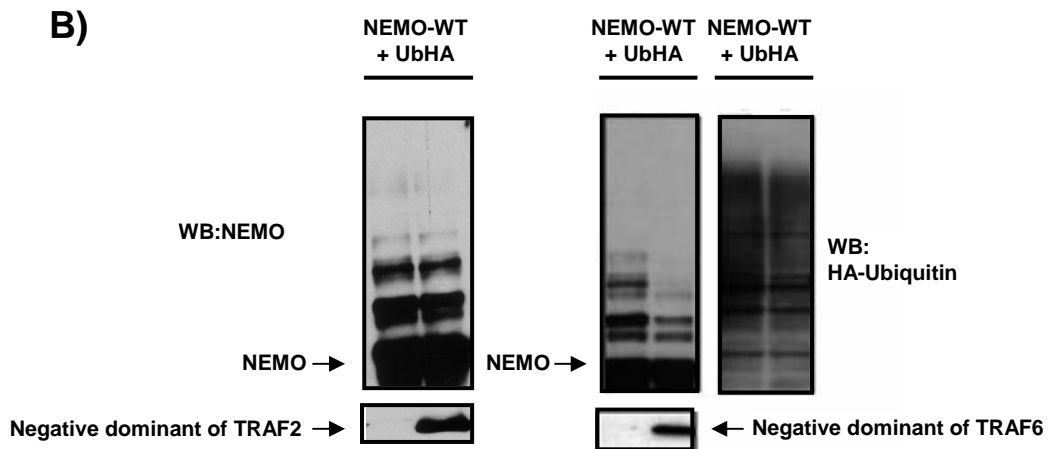
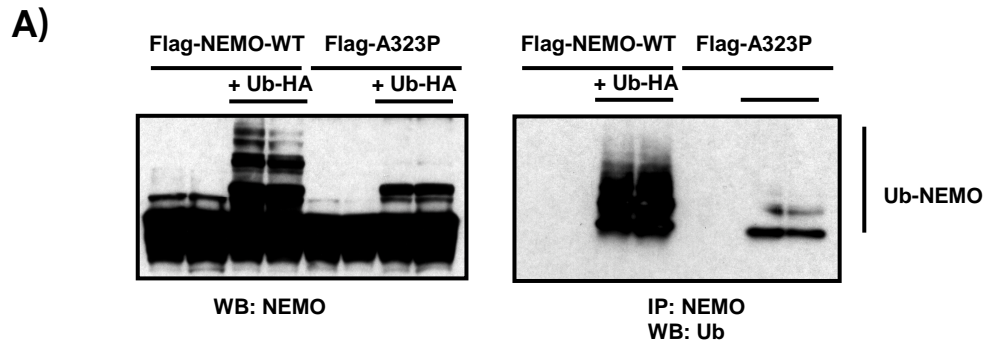
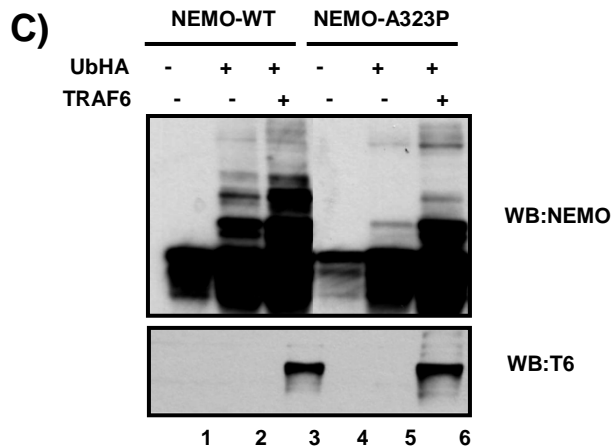


Figure 10
Defective ubiquitination of A323P mutant.

A) Impaired basal ubiquitination of A323P NEMO. HEK 293T cells were transfected with wt NEMO or A323P NEMO alone or with HA-Ub. Cell extracts were analyzed, after western blotting, with anti-hNEMO (left panel) or immunoprecipitated with an anti-NEMO and then analyzed, after western blotting, with anti-HA. Retarded ubiquitinated forms of NEMO are indicated by Ub-NEMO. **B)** Basal ubiquitination of NEMO is TRAF6-dependent. HEK 293T cells were co-transfected with wt NEMO and HA-Ub, without or with a dominant negative version of TRAF6 or TRAF2. Cell extracts were prepared and analyzed, after western blotting, with NEMO, anti-HA or anti-TRAF6.



C) Impaired TRAF6-dependent NEMO ubiquitination caused by A323P mutation. HEK 293T cells were transfected with wt NEMO (lanes 1–3) or A323P NEMO (lanes 4–6). In lanes 2 and 5, NEMO proteins were co-transfected with HA-Ub alone, whereas in lanes 3 and 6 TRAF6 was also included.

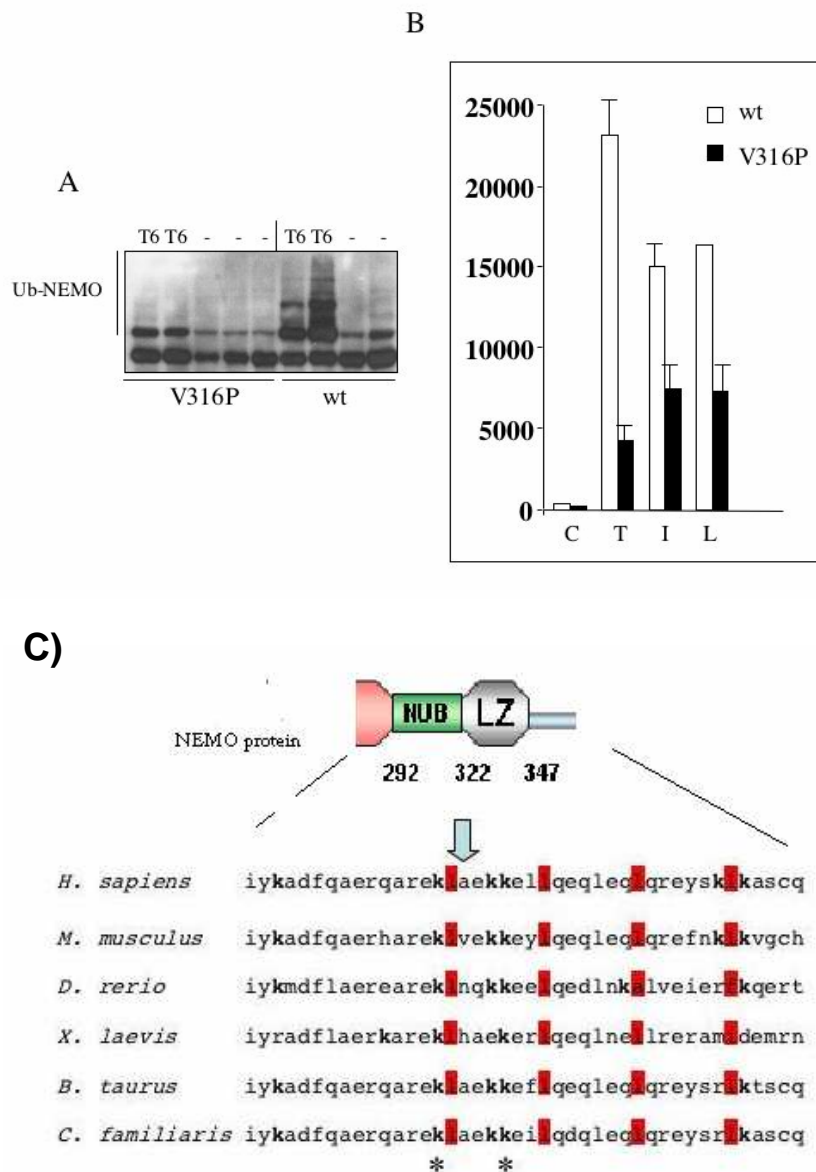


Figure 11
Identification of TRAF6-dependent NEMO ubiquitination sites.

A) Impaired TRAF6-dependent NEMO ubiquitination in murin V316P mutant. **B)** Defective response of murin V316P (corresponding to A323P NEMO) mutant to TNF, IL-1 and LPS. Luciferase assays, using I κ B -Luc as a reporter plasmid, were carried out after complementing NEMO (-) cells. **C)** Conserved lysine residues located in close proximity of A323. NEMO sequences from various species are aligned to indicate the existence of two conserved lysines (asterisks).

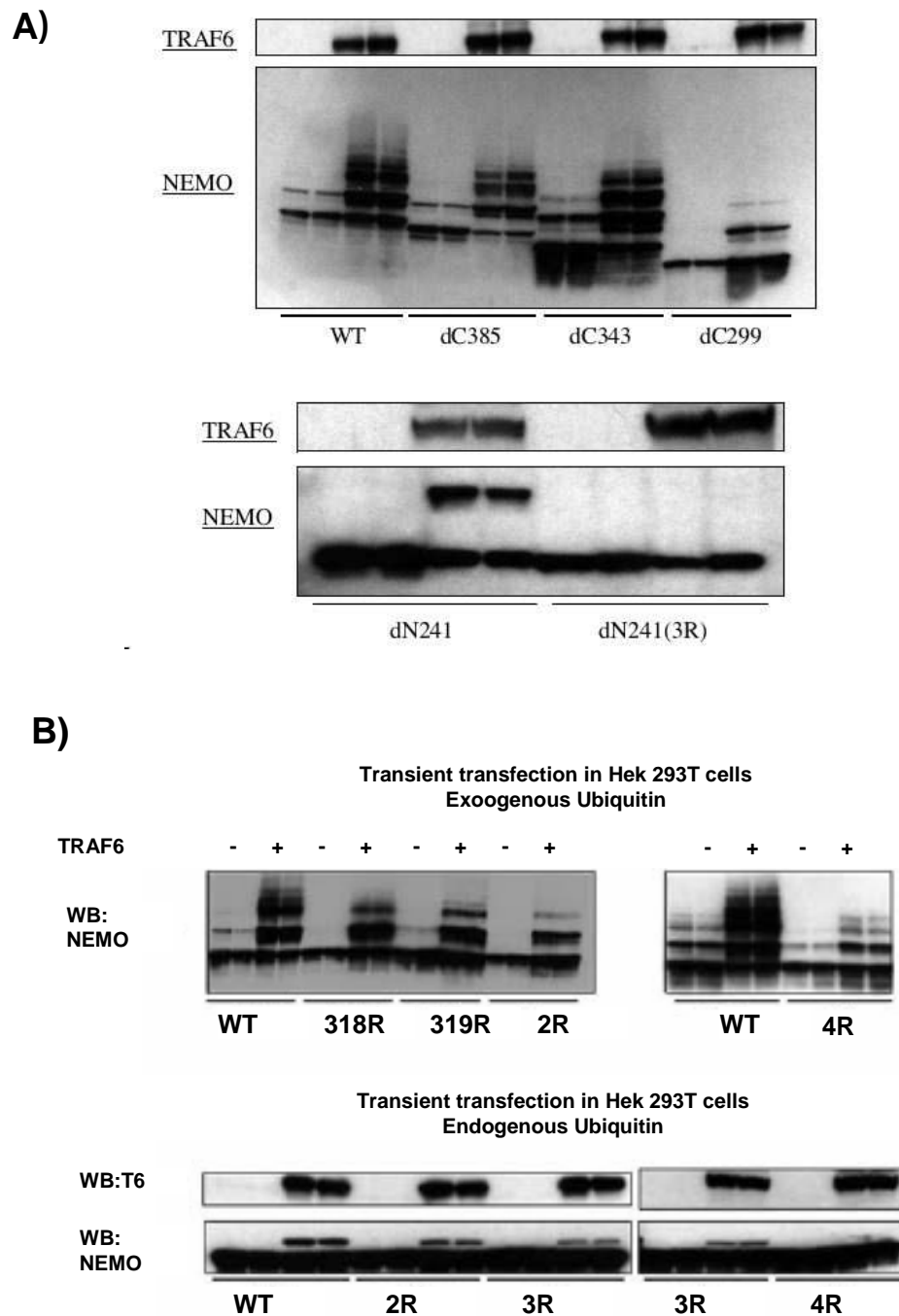
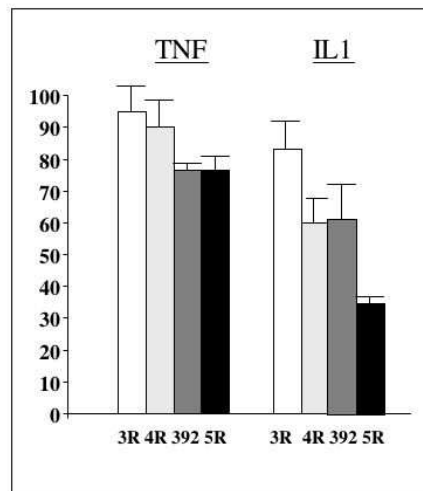
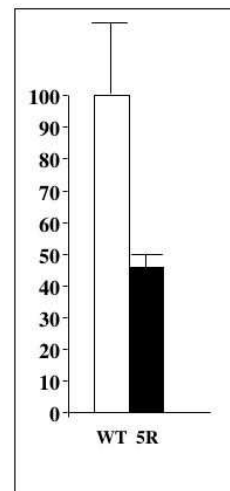
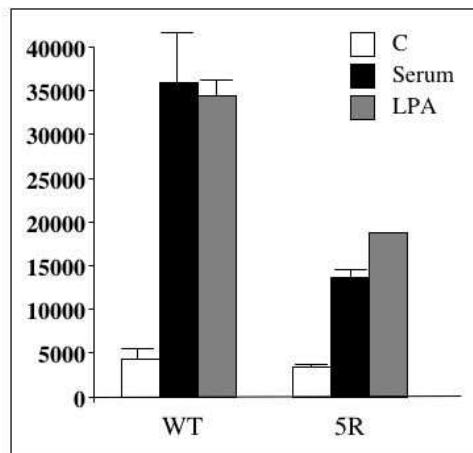


Figure 12

Identification of TRAF6-dependent NEMO ubiquitination sites.

A) Identification of NEMO ubiquitination sites using C-tel (upper panel) an N-ter (lower panel) truncations of NEMO. Various wt and mutated versions of HA-NEMO were co-transfected with HA-Ub alone or with Flag-TRAF6. Cells extracts were analyzed, after western blotting, with anti-NEMO.

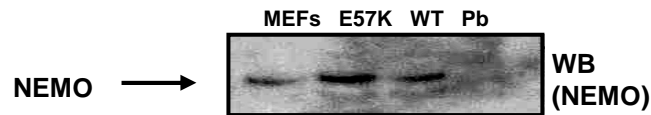
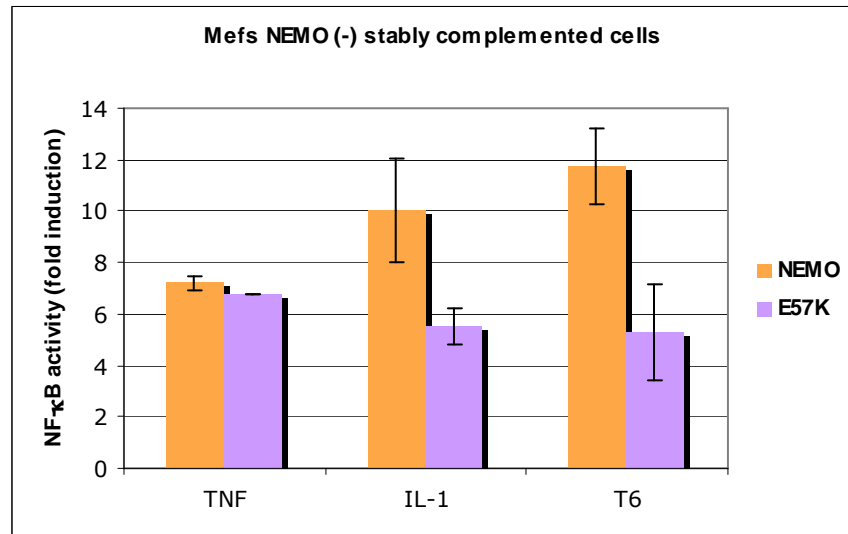
B) Mutagenesis analysis of NEMO ubiquitination sites. The analysis was carried out as described in A) but co-transfecting with Flag-TRAF6 and either with (upper panel) or without HA-Ub (lower panel).

A)**B)****C)****Figure 13****Functional analysis of NEMO ubiquitination sites.**

A) Participation of NEMO ubiquitination in TNF and IL-1 signaling. The analysis was carried out as previously, using complementation of NEMO (-) MEFs with the indicated NEMO mutants. Cells stimulated for 4 h with the indicated stimuli. In **B)** LPS stimulation was shown.

C) Participation of NEMO ubiquitination in NF- κ B activation by serum and LPA. The analysis was carried out as in (A).

A)



B)

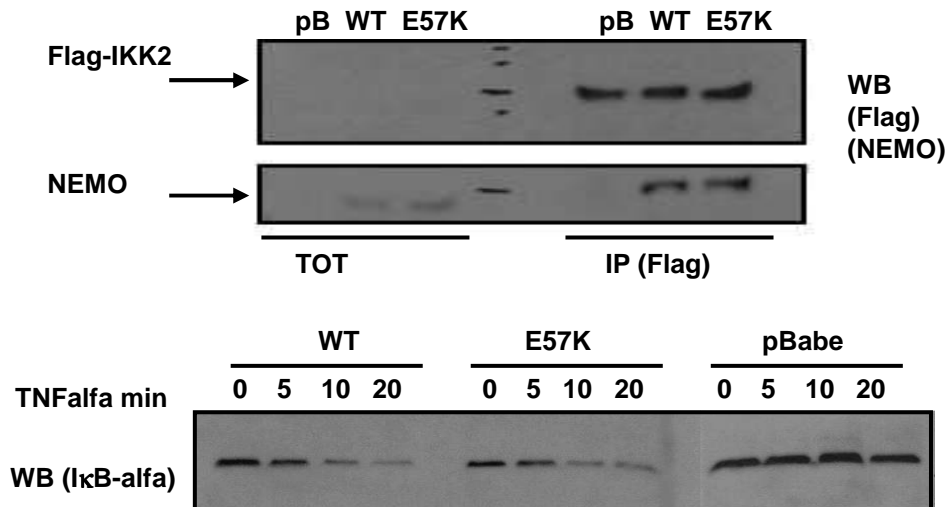


Figure 14

The E57 of NEMO is required for IL-1 mediated NF-κB activation.

A) Expression of MEFs NEMO (-) cells stably complemented with WT NEMO or E57K NEMO (lower panel) and luciferase activity of NF-κB (upper panel) in response to TNF-α, IL-1 (4h of treatment) and TRAF6 overexpression. Error bars represent variation ranges of duplicate experiments. B) MEFs cells stably complemented with NEMO or E57K NEMO were transfected with Flag-IKK2 (upper panel) and the extracts were subjected to anti-flag M2 agarose immunoprecipitation. The coimmunoprecipitated NEMO were analysed by immunoblotting. The cells, as indicated in the lower panel, were stimulated with TNF-α for the indicated time, and then the amount of IκB-α was determined by immunoblotting. pBabe (or pb) represents the empty vector

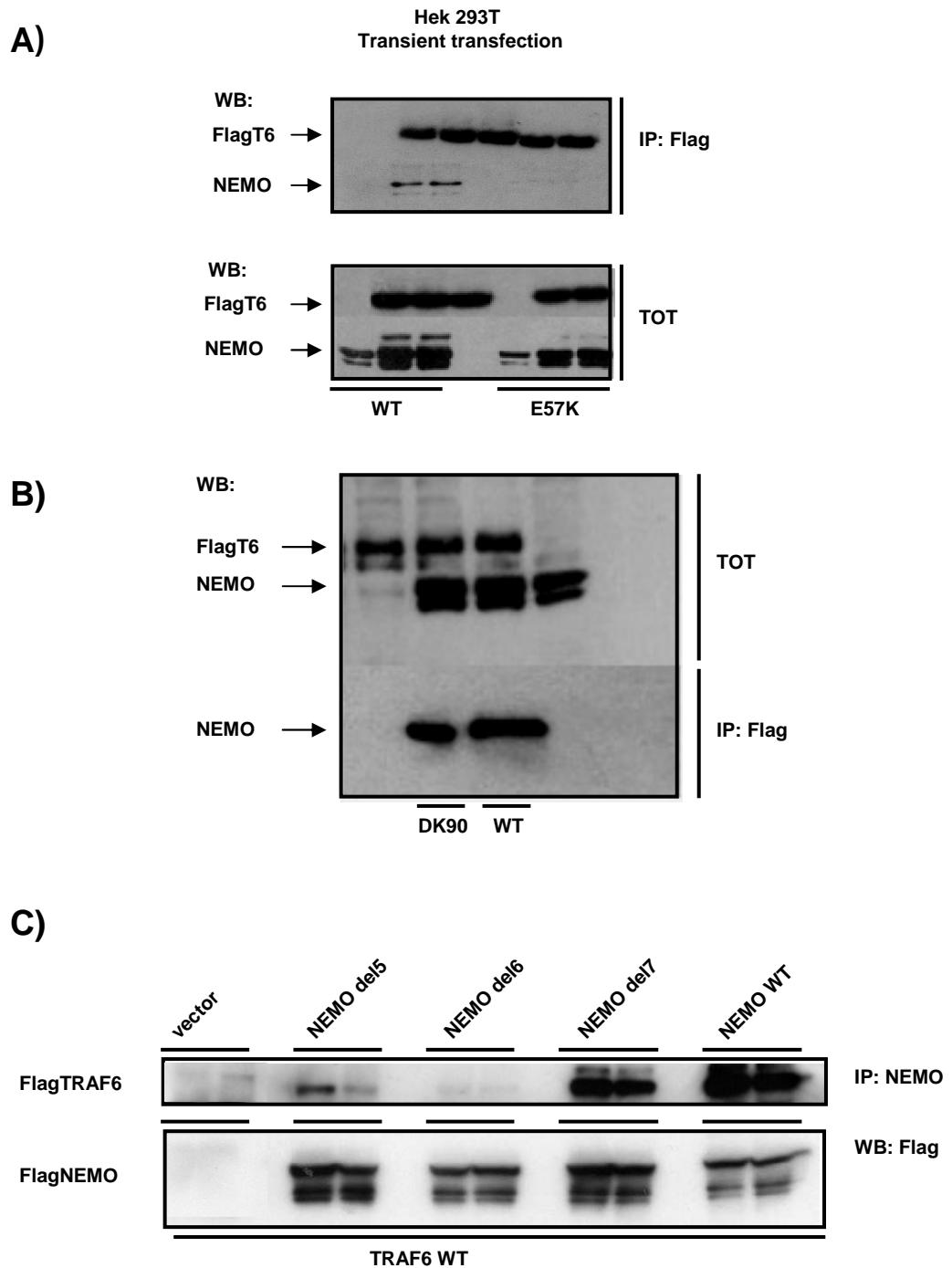


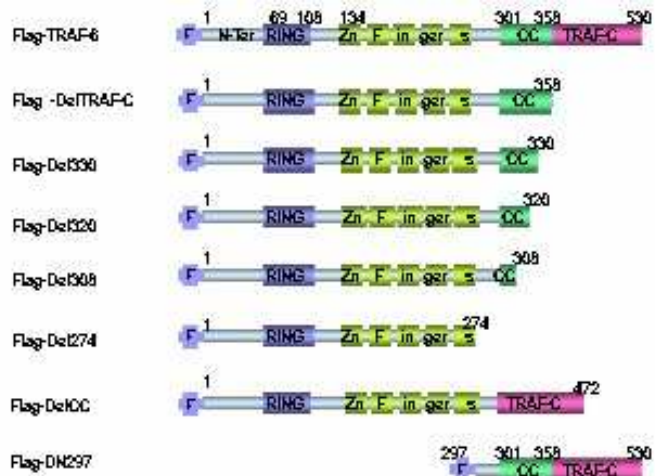
Figure 15

The N-ter domain of NEMO, including E57 residue, is required for the interaction with TRAF6.

A) HEK 293T cells transiently transfected with NEMO or E57K NEMO in combination with FlagTRAF6. The extracts were subjected to anti-flag M2 agarose immunoprecipitation. The coimmunoprecipitated NEMO was analysed by immunoblotting. **B)** Interaction between DK90 NEMO and TRAF6 was analyzed as in A).

C) Various N-terminus deletions of NEMO were co-transfected with Flag-TRAF6. Cells extracts were immunoprecipitated using an anti NEMO and analyzed, after western blotting, with anti-Flag.

A)



B)

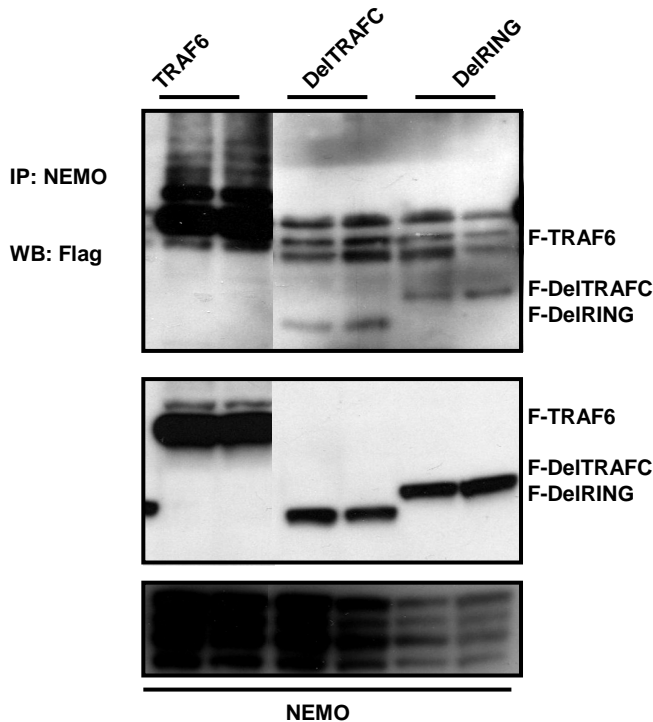
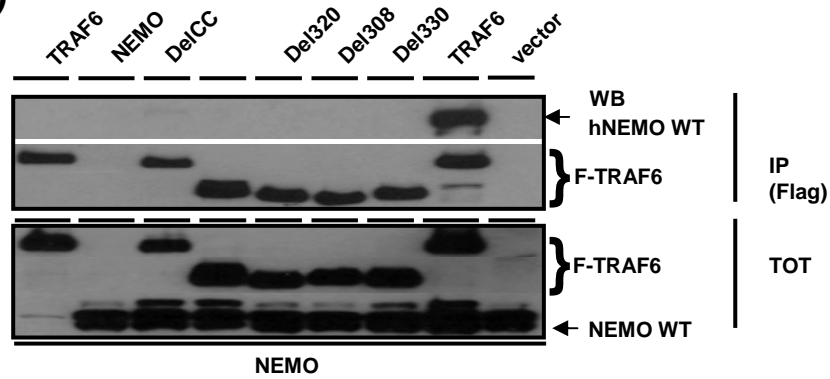
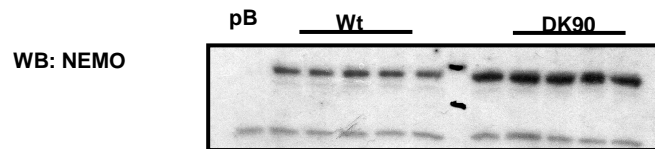
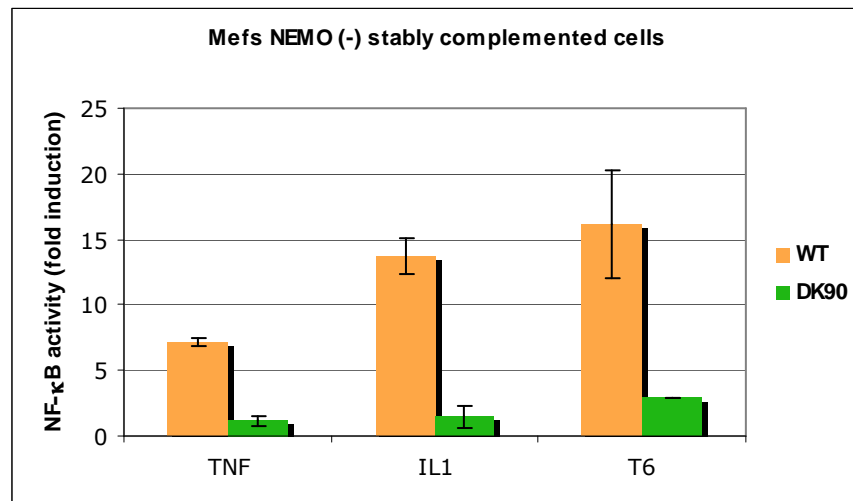


Figure 16
The CC of TRAF6 is required for the interaction with NEMO.

A) Schematic diagrams of TRAF6 and its deletion mutants. The RING, zinc finger, ZF, coiled coil (CC) and TRAF-C domains are shown

B) HEK 293T cells transiently transfected with NEMO in combination with Flag-TRAF6 deletion mutants. The extracts were subjected to anti-flag M2 agarose (upper panel) or anti-NEMO (lower panel) immunoprecipitation. The immunoprecipitated NEMO or Flag-TRAF6 were analysed by immunoblotting.

A)



B)

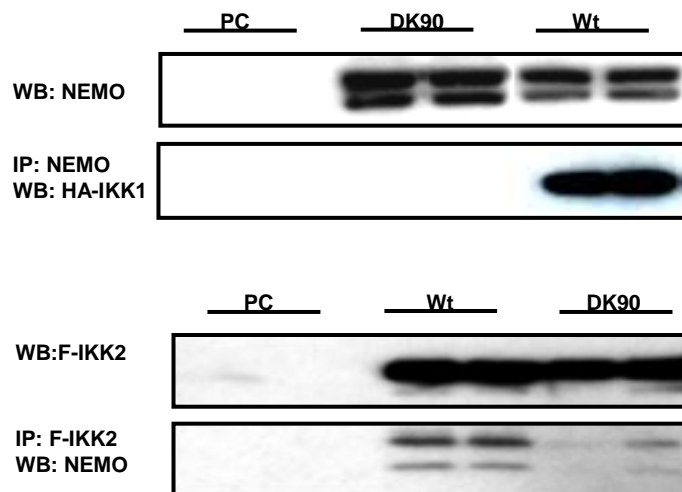


Figure 17

The K90 of NEMO is required for IL-1, TNF and TRAF6-mediated NF- κ B activation.

A) MEFs NEMO (-) cells stably complemented with NEMO or DK90 NEMO luciferase activity of NF- κ B in response to TNF- α , IL-1 (4h of treatment) and TRAF6 overexpression. Error bars represent variation ranges of duplicate experiments. The extracts were subjected to immunoblotting.

B) HEK 293T cells transiently transfected with NEMO or DK90 NEMO in combination with HA-IKK1 (upper panel) and Flag-IKK2 (lower panel). The extracts were subjected to anti-flag M2 agarose or anti-NEMO immunoprecipitation. The immunoprecipitated NEMO or HA-IKK1 were analysed by immunoblotting. Pc represents the empty vector (pcDNA3).